Article:
Foster, J.A., Parker, R.M., Belenguer, A.M. et al. (4 more authors) (2015) Differentially Addressable Cavities within Metal-Organic Cage-Cross-Linked Polymeric Hydrogels. Journal of the American Chemical Society, 137 (30). pp. 9722-9729. ISSN 0002-7863

https://doi.org/10.1021/jacs.5b05507

Supplementary Information for

Differentially Addressable Cavities within Metal-organic Cage-cross-linked Polymeric Hydrogels

Jonathan A. Foster,[†] Richard M. Parker,[†] Ana M. Belenguer,[†] Norifumi Kishi,[‡] Sam Sutton,[†] Chris Abell,[†] Jonathan R. Nitschke*[†]

[†]University of Cambridge, Lensfield Road, Cambridge, CB2 1EW, United Kingdom

[‡] Chemical Resources Laboratory, Tokyo Institute of Technology, 4259 Nagatuta, Midori-ku, Yokohama 226-8502, Japan

Contents

1. Hydrogel synthesis and Characterisation

1.1 General details

Commercial solvents and reagents were used without further purification. All reactions were carried out in dry glassware with a nitrogen overpressure. NMR spectra were recorded on a Bruker Advance DPX 400 or Bruker Advance Cryo 500 spectrometer. Chemical shifts for ^{1}H, ^{13}C, and ^{19}F are reported in ppm on the δ scale; ^{1}H and ^{13}C were referenced to the residual solvent peak, and ^{19}F was referenced to C_6F_6. All coupling constants are reported in Hz. Electrospray Ionization mass spectra (ESI-MS) for the ligands were obtained on a Micromass Quattro LC infused from a Harvard Syringe Pump. The mass spectrometric service for cage **3** were performed by the National Mass Spectrometry Facility at Swansea University using a Thermo Scientific LTQ Orbitrap XL mass spectrometer in negative ionisation mode. Samples were dissolved in water, diluted 1:100 with methanol and infused with an Advion TriVersa NanoMate at a rate of 0.25μL min^{-1}. Elemental analyses were obtained on an Exeter Analytical CE-440 Elemental Analyzer. Scanning Electron Microscopy (SEM) was carried out on a FEI Nova NanoSEM with accelerating voltages of 2-5 keV, samples were splutter coated with platinum (40 mA, 20 s) unless otherwise stated.

1.2 Dialdehyde B, Poly[oxy(ethane-1,2-diyl)]bis(oxy)dipicolinaldehyde

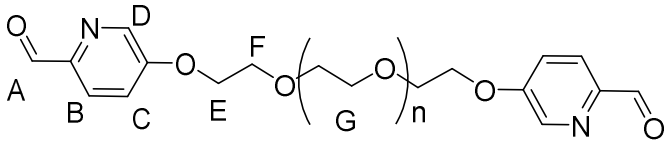

To a round bottom flask was added cesium carbonate (560.9 mg, 1.72 mmol), polyethylene glycol (RMM = 1000 Da, 208.9 mg, 0.21 mmol) and dry dimethylformamide (25 ml). The reaction mixture was stirred at 110°C for 1 h. 5-fluoro-2-formylpyridine (130.9 mg, 1.05 mmol) was added and the reaction was stirred for a further 48 h at 100 °C. The DMF was removed under reduced pressure and the resultant brown oil was dissolved in 50 ml DCM, to which 1 M HCl (aq) (10 mL) was added and the mixture stirred for 10 minutes. Once complete, 4 M NaOH (aq) (30 mL) was added and the organic layer extracted under basic conditions. The organic layer was dried with $MgSO_4$ and concentrated under reduced pressure to afford a brown oil. Excess 5-fluoropyridine could be removed by repeated washing of the oil with diethyl ether. The oil was further dried under high vacuum at 50°C to give dialdehyde **B** (200 mg, 80%) and stored in a freezer at -20˚C until use. ^{1}H NMR (500 MHz, $CDCl_3$) δ/ppm 9.19 (1H, s, **A**), 8.48 (1H, d, J 2.8, **D**), 7.99 (1H, d, 8.8 Hz, **B**), 7.36 (1H, dd, J 8.8, 2.8, **C**), 4.30 (2H, t, J 4.6, **E**), 3.91 (2H, t, J 4.8, **F**), 3.78-3.62 (40 H, m, **G**). ESI-MS (MeOH): m/z 472.6, 516.2, 538.2, 560.3, 582.3, 604.3, 626.3, 648.3, 670.3, 692.4, 714.4 ($[M+2Na - C_6H_3NO]^{2+}$ for n=18-29), 955.5, 999.5, 1043.5, 1087.5, 1131.5, 1175.6, 1219.6, 1263.6, 1307.7, 1351.7, 1395.6 ($[M+2Na]^{+}$ for n=16-26). Elemental calculated for $C_{56}H_{96}N_2O_{25}$: C, 56.17; H, 8.08; N, 2.34. Found: C, 57.06; H, 8.12; N, 2.27

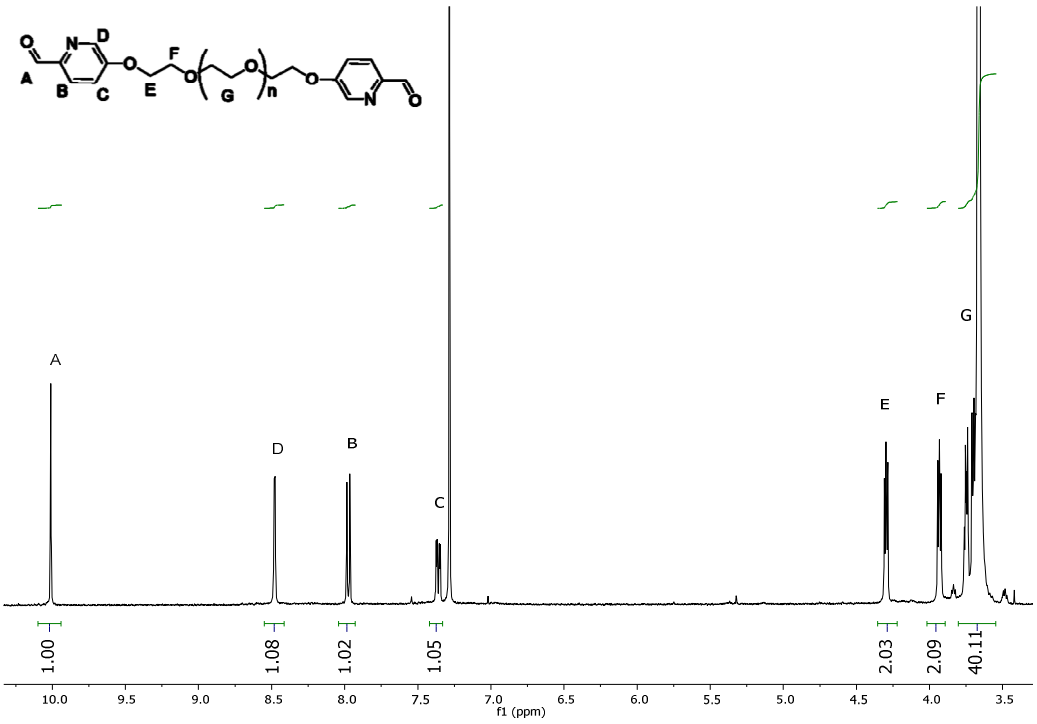

Figure S1: ^{1}H NMR assignment of dialdehyde **B** in $CDCl_3$ highlighting integrals of PEG and aliphatic chains.

1.3 Subcomponent self-assembly of hydrogels

15 wt% hydrogel of cage 2

Tetramethylammonium hydroxide pentahydrate (12.54 mg, 0.069 mmol) was dissolved in 0.4 ml of D_2O and 4,4´-diaminobiphenyl-2,2´-disulphonic acid (86.4%) (14.11 mg, 0.035 mmol) and dialdehyde **B** (41.94 mg, 0.04 mmol) were added to form a dark brown solution. Iron sulphate heptahydrate (6.41 mg, 0.023 mmol) dissolved in 0.1 ml of D_2O was added to the solution and shaken briefly. The solution immediately turned purple and a stiff gel rapidly formed within a period of 1 minute.

10 wt% hydrogels of cage 2

Tetramethylammonium hydroxide pentahydrate (8.36 mg, 0.046 mmol) was dissolved in 0.4 ml of D_2O and 4,4´-diaminobiphenyl-2,2´-disulphonic acid (86.4%) (9.41 mg, 0.023 mmol) and dialdehyde **B** (27.96 mg, 0.023 mmol) were added to form a dark brown solution. Iron sulphate heptahydrate (4.27 mg, 0.023 mmol) dissolved in 0.1 ml of D_2O was added to the solution and shaken briefly. The solution immediately turned purple and a stiff gel formed within a period of 5 minutes.

5 wt% solution of cage 2

Tetramethylammonium hydroxide pentahydrate (4.18 mg, 0.023 mmol) was dissolved in 0.4 ml of D_2O and 4,4´-diaminobiphenyl-2,2´-disulphonic acid (86.4%) (4.70 mg, 0.012 mmol) and dialdehyde **B** (13.98 mg, 0.012 mmol) were added to form a dark brown solution. Iron sulphate heptahydrate (2.14 mg, 0.008 mmol) dissolved in 0.1 ml of D_2O was added to the solution and shaken briefly. The solution immediately turned purple however no gels were observed.

Conversion of 5 wt% solution of cage 2 to 15 wt% hydrogel

1.2 ml of a 5 wt% solution of cage **2** was added to a vial, frozen in liquid nitrogen and freeze dried for 6 h to give a fibrous xerogel. 0.4 ml of water was added and the xerogel initially swelled to form a

hydrogel before fully dissolving to give a purple solution. After 2 days at room temperature, the sample was observed to have formed a hydrogel which was stable with respect to inversion.

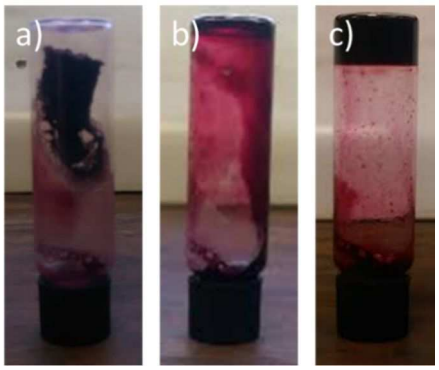

Figure S2 Photograph of a 5 wt% solution of cage **2** following a) freeze drying, b) the addition of 0.4 ml water, c) after 2 days

15 wt% corner complex

Tetramethylammonium hydroxide pentahydrate (12.88 mg, 0.071 mmol) was dissolved in 0.4ml of D_2O and 4-aminophenyl-2 sulphonic acid (12.30 mg, 0.071 mmol) and dialdehyde **B** (43.09 mg, 0.036 mmol) were added to form a dark brown solution. Iron sulphate heptahydrate (6.41 mg, 0.024 mmol) dissolved in 0.1 ml of D_2O was added to the solution and shaken briefly. The solution immediately turned purple but no hydrogel was observed to form.

1.4 Rheometry

The mechanical properties of the hydrogels were tested using a TA Instruments Advanced Rheometer 2000 equipped with a peltier heating plate. A 40 mm anodised aluminium flat plate geometry was used with a gap of 500 µm. All tests were done immediately after transferring 0.5 ml of a preformed 15 wt% hydrogel onto the sample stage. Measurements were made using an oscillatory strain of 1%, a frequency of 10 rad/s and a temperature of 25°C while measuring the storage (G′) and loss modulus (G″) unless otherwise stated.

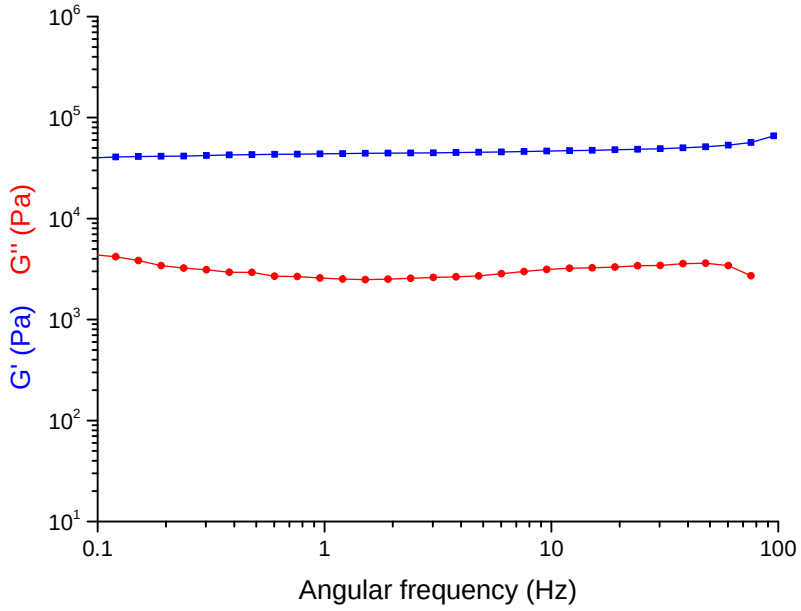

Figure S3 Plot showing frequency dependency of 15 w% hydrogels of cage **2**. The values for the elastic modulus G′ (blue) and storage modulus G″ (red) are plotted. Measurements were taken at 25°C with a fixed oscillatory strain of 0.1%.

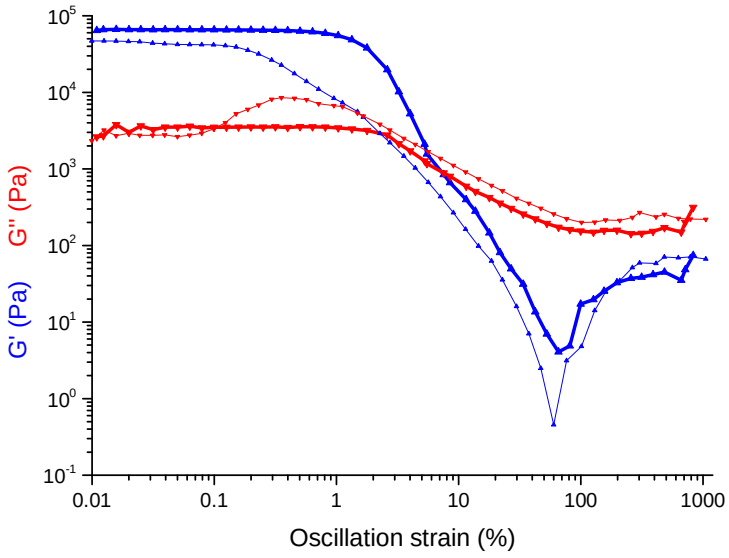

Figure S4: Strain sweep for 15 wt% hydrogels of cage **2**. Oscillatory strain was gradually increased (bold lines) then decreased (thin lines) from 0.1% then 200% the values for the elastic modulus G′ (blue) and storage modulus G″ (red) are plotted. Measurements were taken at 25°C with a fixed frequency of 10 rad/s.

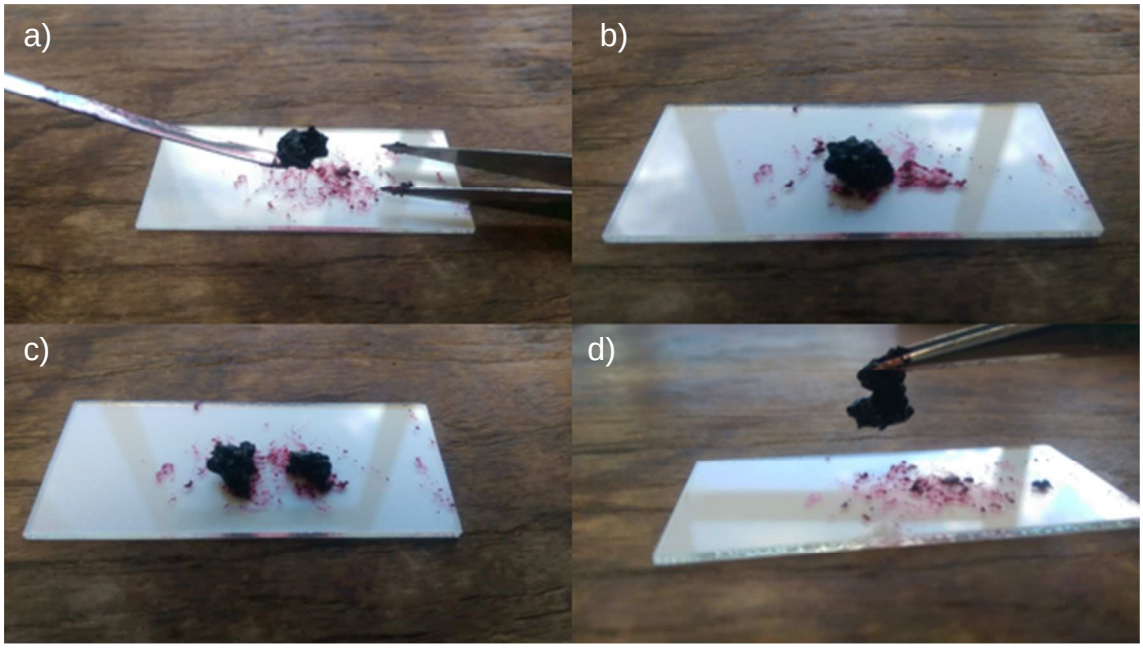

Figure S5 Figure showing self-healing behaviour of 15 wt% hydrogel of cage **2**. The hydrogel was (a) scooped from a vial, (b) placed on a glass slide, (c) cut in two with a spatula, (d) the two pieces were brought back together and the self-healing process occurred instantaneously allowing the healed hydrogel to support its own weight.

1.5 Scanning electron microscopy

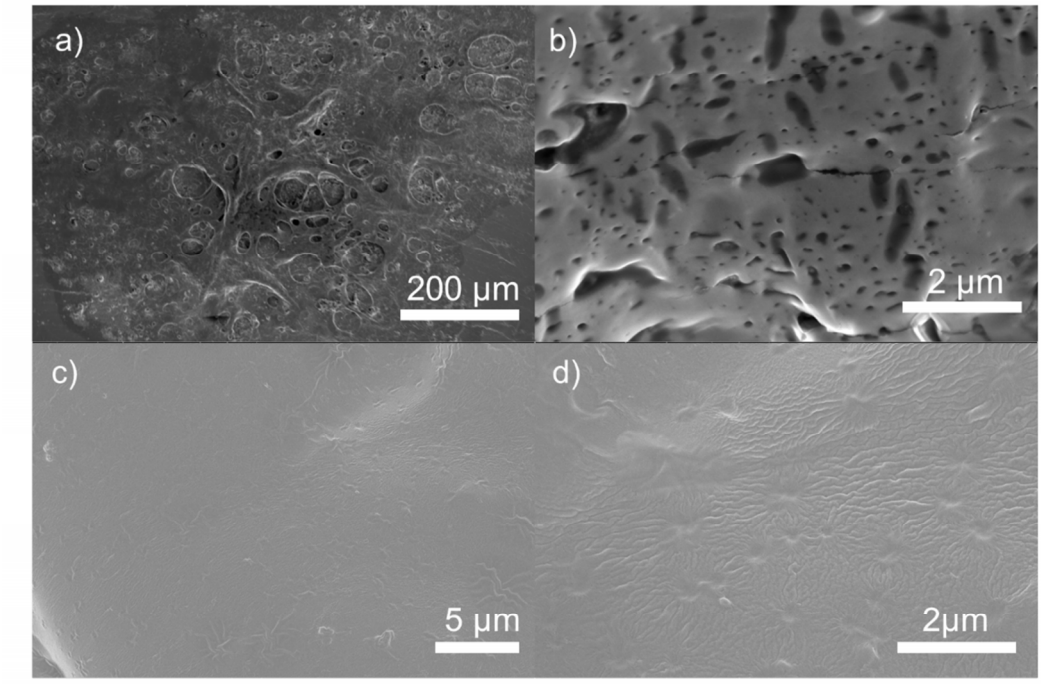

Figure S6: SEM images showing xerogels deposited onto aluminium pins and either (a/b) freeze dried then splutter coated with platinum (20 s, 40 mA) or (c/d) dried in air at room temperature and splutter coated with platinum (10 s, 40 mA). High resolution imaging of uncoated samples was not possible due to charging effects.

2. Guest binding studies

2.1 Monoaldehyde C, 5-(2-(2-(2-methoxyethoxy)ethoxy)ethoxy)picolinaldehyde

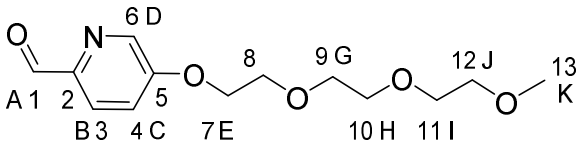

5-(2-(2-(2-methoxyethoxy)ethoxy)ethoxy)picolinaldehyde**:** To a round bottom flask was added cesium carbonate (500.9 mg, 1.54 mmol), triethyleneglycol monomethylether (100.97 mg, 0.61 mmol) and dry dimethylformamide (25 ml). The reaction mixture was stirred at 100°C for 1 h. 5-fluoro-2-formylpyridine (105.8 mg, 0.85 mmol) was added and the reaction was stirred for a further 18 h at 100°C. The DMF was removed under reduced pressure and the resultant brown oil was dissolved in 50 ml DCM, to which 1 M $HCl_{(aq)}$ (10 mL) was added and the mixture stirred for 10 minutes. 4 M NaOH (30 mL) was added and the organic layer extracted under basic conditions. The organic layer was dried with $MgSO_4$ and concentrated under reduced pressure to afford monoaldehyde **C** as a brown oil (128 mg, 77%) and stored in a freezer at -20˚C until use. ^{1}H NMR (400 MHz, $CDCl_3$-d) δ/ppm 10.00 (s, 1H, **A**), 8.47 (d, J = 2.7 Hz, 1H, **D**), 7.96 (d, J = 8.7 Hz, 1H, **B**), 7.35 (dd, J = 8.6, 2.7 Hz, 1H, **C**), 4.33 – 4.22 (m, 2H, **E**), 3.96 – 3.90 (m, 2H, **F**), 3.78 – 3.53 (m, 8H, **G-J**), 3.39 (s, 3H, **K**). ^{13}C NMR{^{1}H} 192.04 (**1**), 158.34 (**2**), 146.39 (**5**), 138.92 (**6**), 123.30 (**3**), 120.70 (**4**), 71.92 (**12**), 70.96 (**9**), 70.66 (**10**), 70.61 (**11**), 69.39 (**8**), 68.23 (**7**), 59.06 (**13**). ESI-MS (MeOH): 165.08 (35%, $[M\text{-}C_6H_4NO]^+$), 165.08 (25%, $[M\text{-}C_6H_4NO\text{+}Na]^+$) 270.8 (100%, $[M+H]^+$). Elemental calculated for $C_{13}H_{19}NO_5$: C, 57.98; H, 7.11; N, 5.20. Found: C, 57.93; H, 7.14; N, 5.24

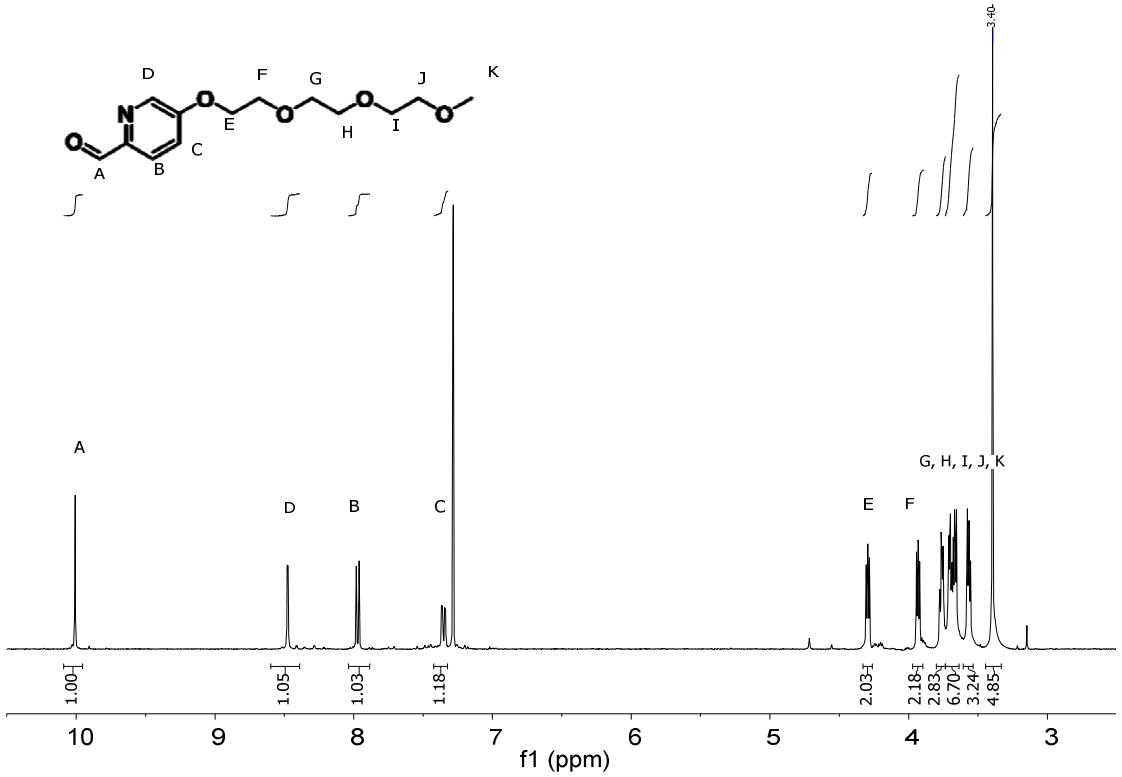

Figure S7: ^{1}H NMR assignment for monoaldehyde **B**

2.2 Model cage 3

Tetramethylammonium hydroxide pentahydrate (50.16 mg, 0.28 mmol, 12 eq.), 4,4´-diaminobiphenyl-2,2´-disulphonic acid (86.4%) (56.45 mg, 0.14 mmol, 6 eq.) and monoaldehyde **C** (43.09 mg, 0.28 mmol, 12 eq) were dissolved together in 1.5 ml D_2O to form a dark brown solution. Iron sulphate heptahydrate (25.65 mg, 0.09 mmol, 4 eq.) was dissolved in 0.5 ml of D_2O and the two solutions were mixed together resulting in a deep purple solution. The mixture was separated equally into four NMR tubes, the solutions were degassed and left for 1 week at room temperature to give model cage **3**. ^{1}H NMR (400 MHz, D_2O) δ 10.00 (s, 1H, **A**), 8.47 (d, J = 2.7 Hz, 1H, **D**), 7.96 (d, J = 8.7 Hz, 1H, **B**), 7.35 (dd, J = 8.6, 2.7 Hz, 1H, **C**), 4.33 – 4.22 (m, 2H, **E**), 3.96 – 3.90 (m, 2H, **F**), 3.78 – 3.53 (m, 8H, **G-J**), 3.39 (s, 3H, **K**). ESI-MS (H_2O/MeOH): 343.0062 (100%, $[C_{12}H_{11}N_2O_6S_2]^-$), 416.0951 (24%, $[C_{16}H_{22}N_3O_6S_2]^-$), 594.1212 (8%, $[C_{25}H_{28}N_3O_{10}S_2]^-$), 1323.5317 (34%, $[\mathbf{3}]^{4-}$), 1789.7431 (8%, $[\mathbf{3} + NMe_4]^{3-}$),

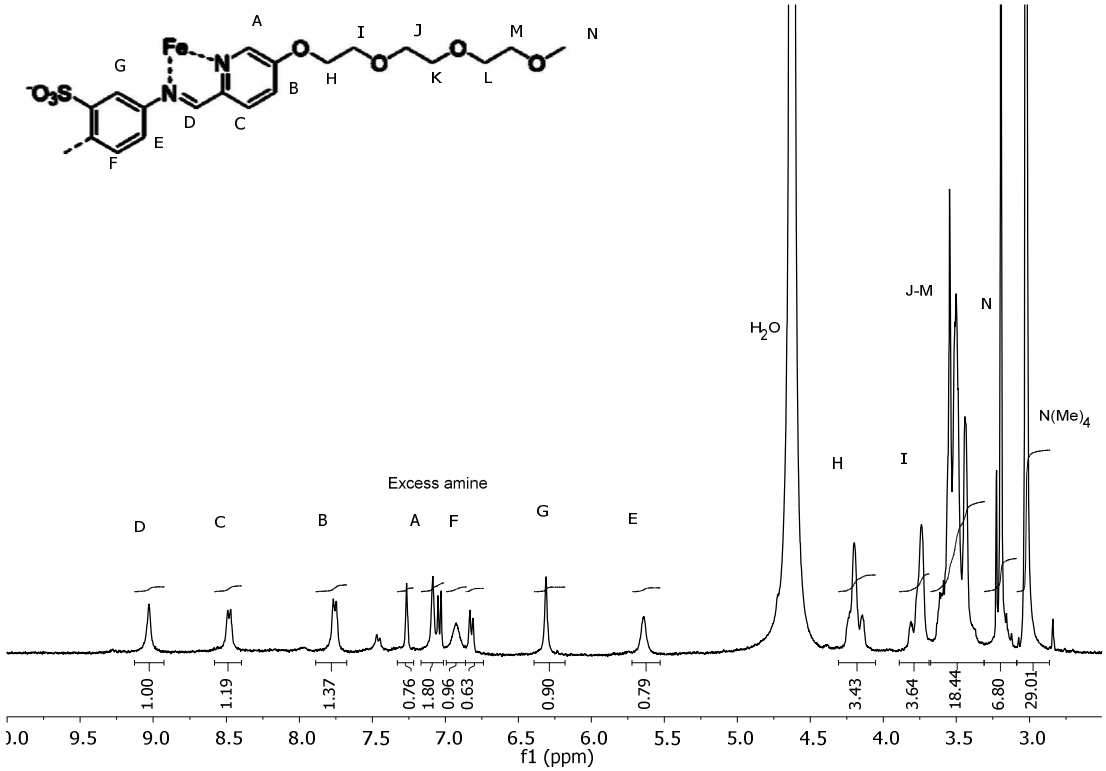

Figure S8: NMR showing the structure of cage **3**.

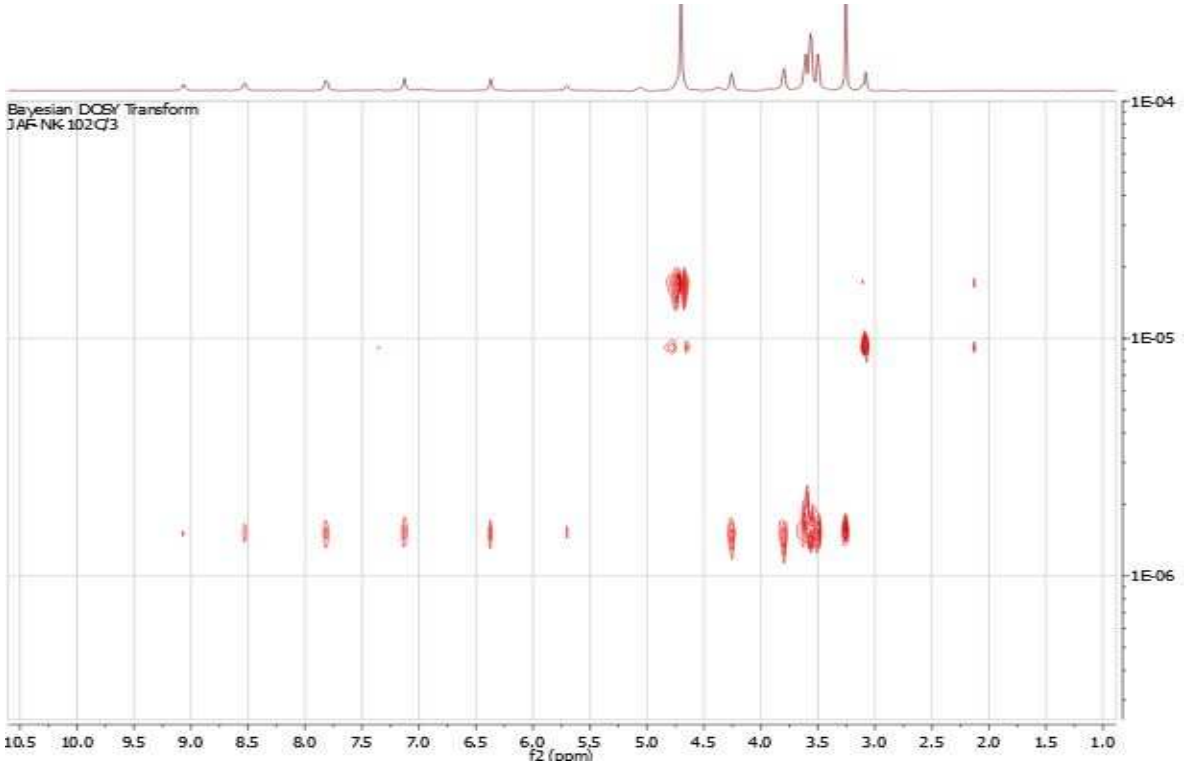

Figure S9: DOSY NMR showing diffusion of cage **3** in D_2O.

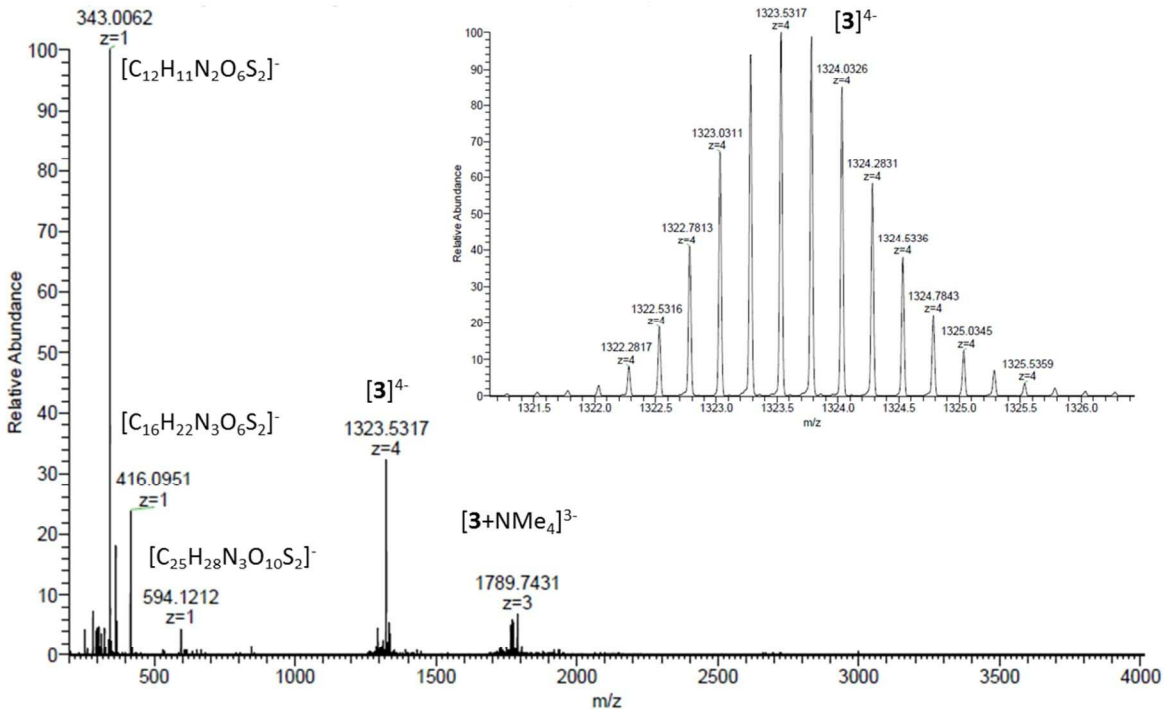

Figure S10: Mass spectrum showing cage **3**, insert shows high resolution spectrum for cage **3**.

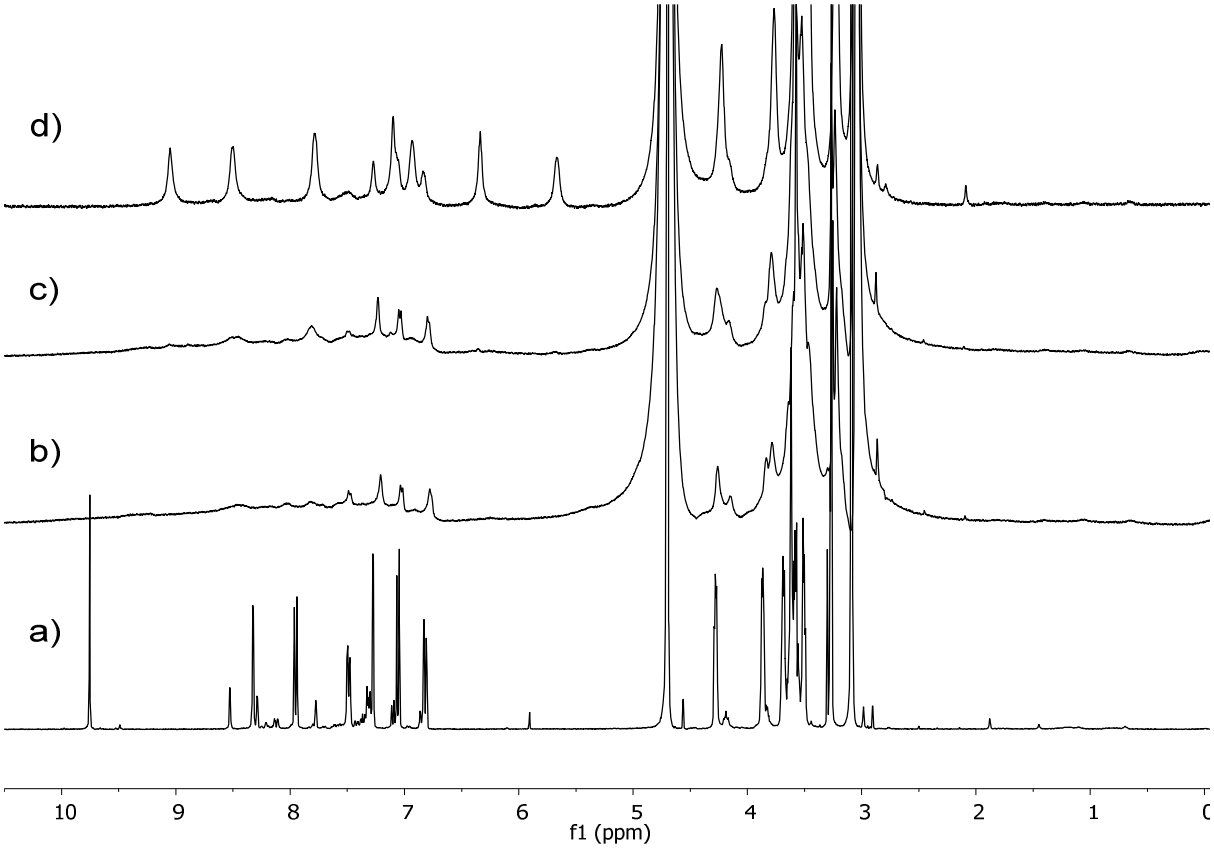

Figure S11: Showing formation of cage **3**; a) mixture of cage components except iron in D_2O and following the addition of iron after b) 1 minute, c) 1 h and d) 4 days at room temperature.

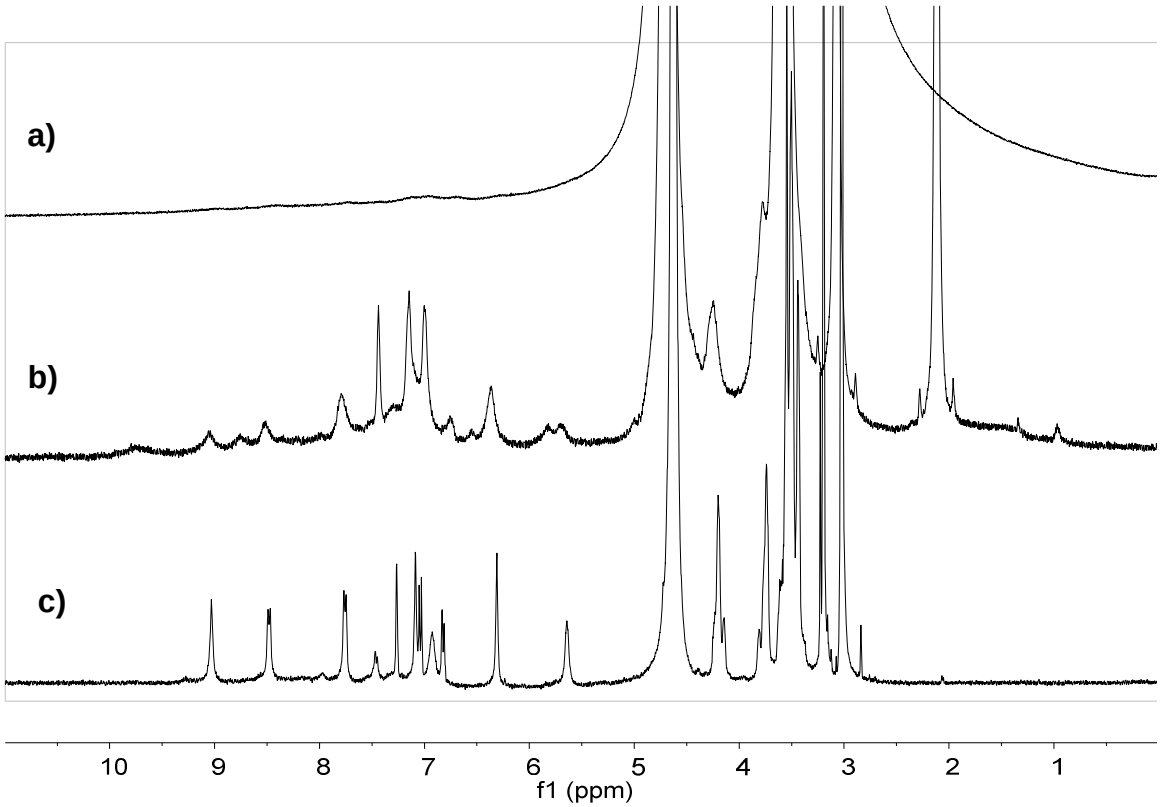

Figure S12: ^{1}H NMR spectra for a) 15wt% hydrogel of cage **2** in D_2O b) 5 wt% solution of cage **2** and c) cage **3**

2.3 Binding of fluorobenzene to cage complexes

Samples were prepared as outline in section 1.3 and 2.1 in J. Young NMR tubes using 0.4 mL of D_2O to which 2 µL of a 1:1 molar mixture of fluorobenzene:hexafluorobenzene had been added.

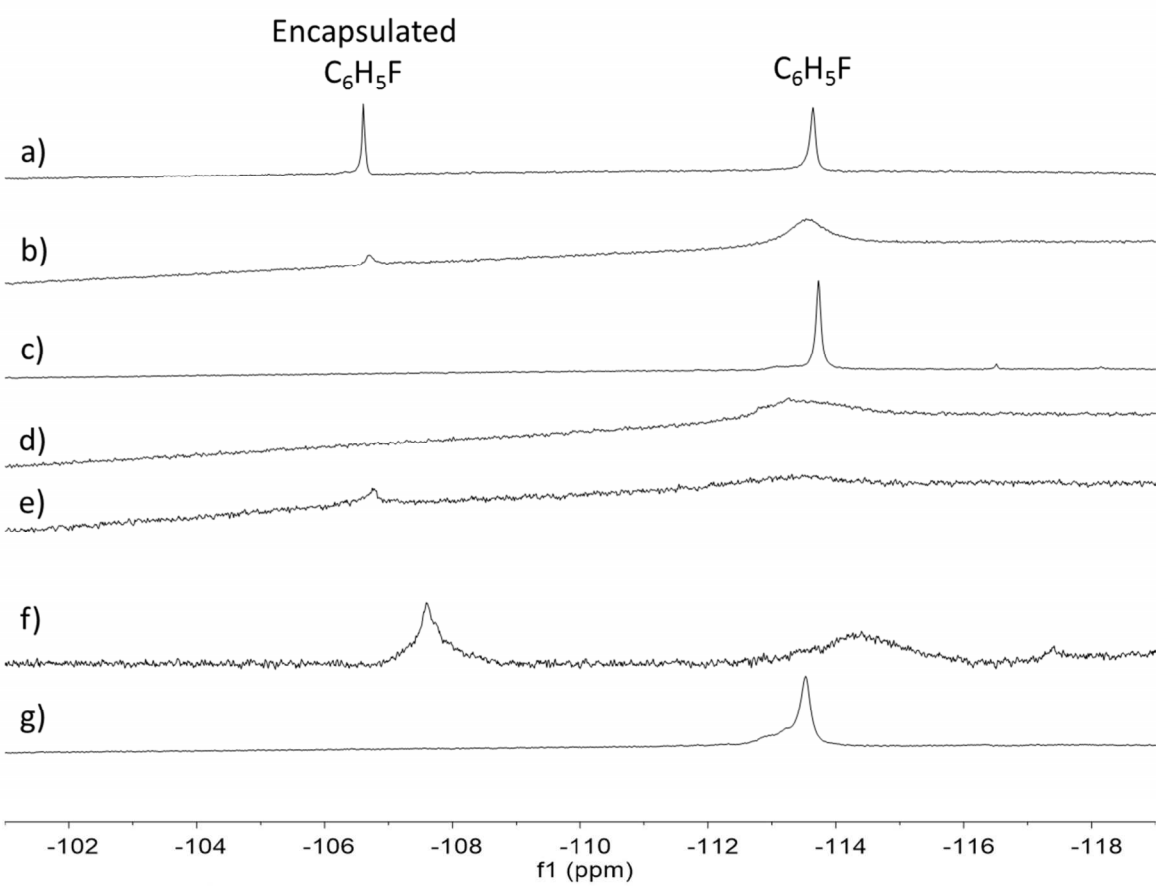

Figure S13: ^{19}F NMR spectra showing behaviour of a 1:1 molar mixture of fluorobenzene:hexafluorobenzene in the presence of a) cage **3** b) 5 wt% solution of cage **2** c) 15 wt% solution of all components of cage **2** except iron, d) 1 h after the addition of iron to make a 15 wt% hydrogel, e) a 1 week old 15 wt% hydrogel of cage **2**, f) a month old 15 wt% hydrogel of cage **2** to which excess fluorobenzene mixture has been infused overnight, g) 15 wt% corner complex formed with aminosulfonate.

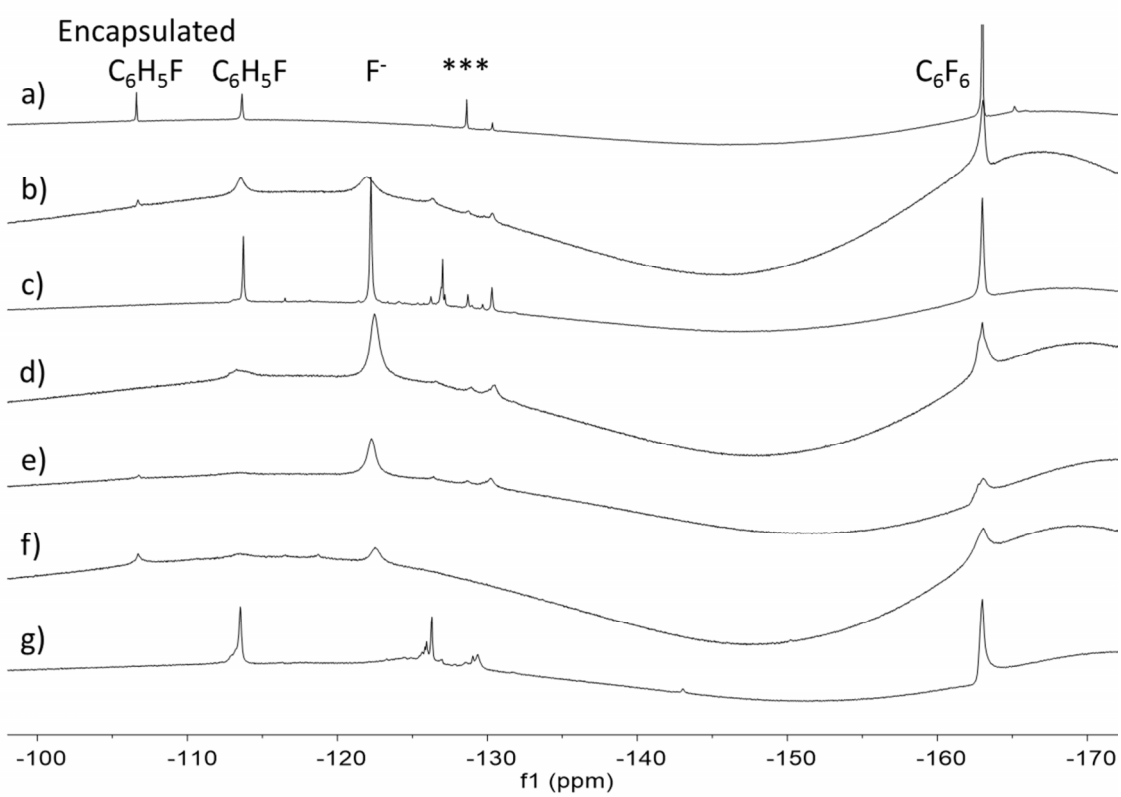

Figure S14: ^{19}F NMR spectra showing behaviour of a 1:1 molar mixture of fluorobenzene:hexafluorobenzene in the presence of a) cage **3** b) 5 wt% solution of **2** c) 15 wt% solution of all components of **2** except iron, d) 1 h after the addition of iron to make a 15 wt% hydrogel, e) a 1 week old 15 wt% hydrogel of **2**, f) a month old 15 wt% hydrogel of **2** to which excess fluorobenzene mixture has been infused overnight, g) 15 wt% corner complex formed with aminosulfonate. A number of impurities were present in the samples, most prominently fluoride (F^-) and a number of peaks (*) that were also present in the 5-fluoro-2-formylpyridine starting material.

3. Guest release studies

3.1 General methods

The experiment was designed to compare the rate of release of chemical species which can act as a guest for the cages in the presence and absence of a competing guest. Benzene, anisole and furan were chosen as guest, non-guest and competing guest species respectively as they possess a chromophore enabling them to be detected by HPLC using a UV-Vis detector.

In the initial experimental design, hydrogel samples were prepared using saturated solutions of either benzene or anisole in order to maximise the initial concentration of guest in the hydrogels and stored in larger vials saturated with benzene in order to prevent evaporation. However, tests on both these hdyrogel sample and reference samples prepared in this way but containing no gelator all showed an increase in benzene and anisole concentration over a period of ~90 mins. This was attributed to the poor solubility of benzene and anisole in water resulting in reservoirs of benzene sticking to the glass walls of the vials and gradually slowly releasing into solution. Attempts to remove the excess benzene by repeated washing methods were unsuccessful. The hydrogel samples were therefore freeze dried in order to remove the excess benzene and furan.

3.2 Hydrogel preparation protocol

1. Stock solutions of HPLC grade water saturated with anisole (solution A 0.0147 M) and benzene (solution B 0.0229 M) were prepared in 100 ml class A volumetric flasks and stirred over night to ensure saturation. A turbid solution of anisole was obtained but addition of 1 ml deionized water resulted in a clear solution which was used.
2. Dialdehyde **B** (167.74 mg, 0.138 mmol, 6 eq.) was weighed into a glass vial, 1 mL of stock solution A or B was added and vortexed to ensure dissolution (no sonication).
3. Tetramethylamonium hydroxide pentahydrate (250.8 mg, 1.384 mmol, 12 equivalents), 4,4′-diaminobiphenyl-2,2′-disulphonic acid (282.3 mg, 0.692 mmol, 6 eq.) and iron(II) sulfate heptahydrate (128.2 mg, 0.461 mmol, 4 eq.) were weighed into separate vials.
4. 5 mL of solution A or B, measured using a 5 ml class A volumetric flask, was added to the vial containing tetramethylammonium, capped (plastic) and briefly sonicated to dissolve. This solution was transferred to the vial containing the diamine, snap-capped and sonicated until a clear solution was obtained. This solution was then transferred to the vial containing iron(II) sulfate, capped (plastic) and briefly mixed and sonicated to dissolve.
5. 125 µL aliquots of this solution were added to individual 1.9 mL scre closure glass HPLC vials using a 200 µl air displacement pipette.
6. 125 µL aliquots of the corresponding dialdehyde **B** solution was pipetted into the same vials and purple hydrogels were observed to rapidly form.
7. The vials were immediately capped (blue screw cap), placed in a sealed vial containing drops of either benzene or anisole to maintain saturation, and stored at room temperature for at least 1 month before use.
8. Reference samples containing only stock solutions A and B were prepared in the same way but without the addition of gel forming subcomponents.
9. Hydrogel samples were frozen in liquid nitrogen and freeze dried for two nights to produce xerogels.

3.3 Release monitoring protocol

10. Stock solutions containing furan (0.01 M) or a 1:1 mixture of benzene and anisole (0.05 M of each) were prepared in 100 ml class A volumetric flask and stirred overnight at RT.

11. Six dried hydrogel samples were resolvated with 0.25 ml of the 1:1 benzene:anisole solution and stored for 1 h at RT along with two reference vials containing only 0.25 ml of benzene/anisole solution.

12. An HPLC programme, designed to take 10 µl aliquots of sample every 2 minutes and measure by UV-vis the concentration of either benzene or anisole in the sample, was started.

13. The cap of the vial containing the first hydrogel was removed and 1.65 mL of a 0.01 M furan solution was added to the vial using a 5,000 µl air displacement pipette with plastic tips.

14. 1.65 mL of the furan solution was added to two further hydrogel samples and a reference vial at two minute intervals then 1.65 mL of deionized water was added to the remaining four samples in the same way.

15. Regular measurements were taken over a period of several hours and samples were mixed continuously between HPLC measurements using rollers to ensure homogeneity and white tak was placed over the HPLC vial cap to minimise solvent loss through holes punctured in the HPLC vial cap by the HPLC needle.

16. Once measurements indicated that the concentration of benzene and anisole had equilibrated (after several hours, see individual experiments for times), the HPLC liquid handling robot was used to inject a set volume of neat furan into the HPLC vials made with deionized water. The corresponding volume of deionized water was added in the same way to the HPLC vials made with furan solution.

In the first experiment (section 3.4), hydrogel samples which had been prepared using saturated benzene solutions were used. This resulted in the release of higher than expected concentrations of benzene from the hydrogel samples, indicating that benzene remained encapsulated within the gel cavities during lyophilisation. During the second experiments (Section 3.5), hydrogel samples which had been formed using saturated anisole solutions were used and the final concentrations of the solutions matched those expected from the reference samples. This result indicates that anisole was not encapsulated and was removed during lyophilisation. No release profile corresponding to dissolution of benzene or anisole from the walls of the vial was observed in any of the reference or hydrogel samples.

3.4 Guest release study 1

The chemical composition of the supernatant above the hydrogels were analyzed by reverse phase HPLC using a modular Agilent 1100 Series HPLC system composed of a HPLC high pressure binary pump, autosampler with injector programming capabilities, column oven with 6 µL heat exchanger and a Diode Array Detector with a semimicro flow cell to reduce peak dispersion when using short columns as in this case. The flow-path was connected using 0.12 mm ID stainless steel tubing to minimize peak dispersion. Methanol and water used to perform this analysis were HPLC grade purchased from Fisher Scientific.

Separation was achieved with an HPLC column (Spherisorb ODS(2) 3 µm 4.6x50 mm) heated to 50˚C using an isocratic 40% methanol in water with a flow rate of 3 ml/min with 10 µL injection volume. UV-vis measurements were taken using an UV detector at wavelengths of 210 nm (8 nm), 217 nm (8 nm), 230 nm (16 nm), 254 nm (16 nm) against a reference at 550 nm (100 nm). Integration of the peak areas was undertaken using Agilent ChemStation software (Rev. B.04.01 [481]).

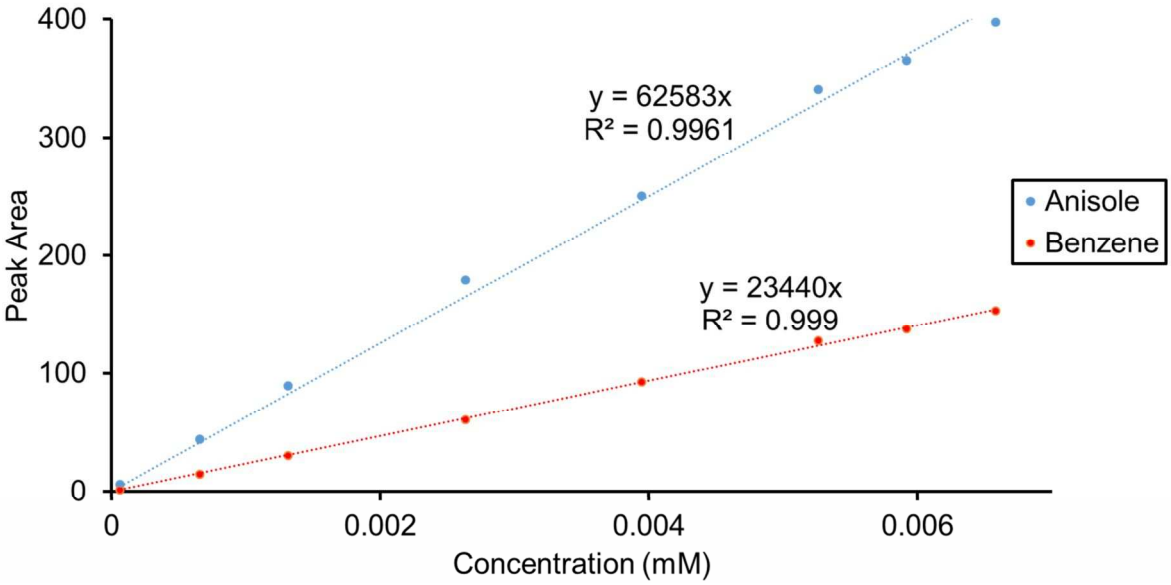

Figure S15: Calibration plot showing peak area at 210 nm against concentration for benzene (blue) and anisole (red) aqueous solutions. Correction factors were used to convert peak areas into concentration (mM).

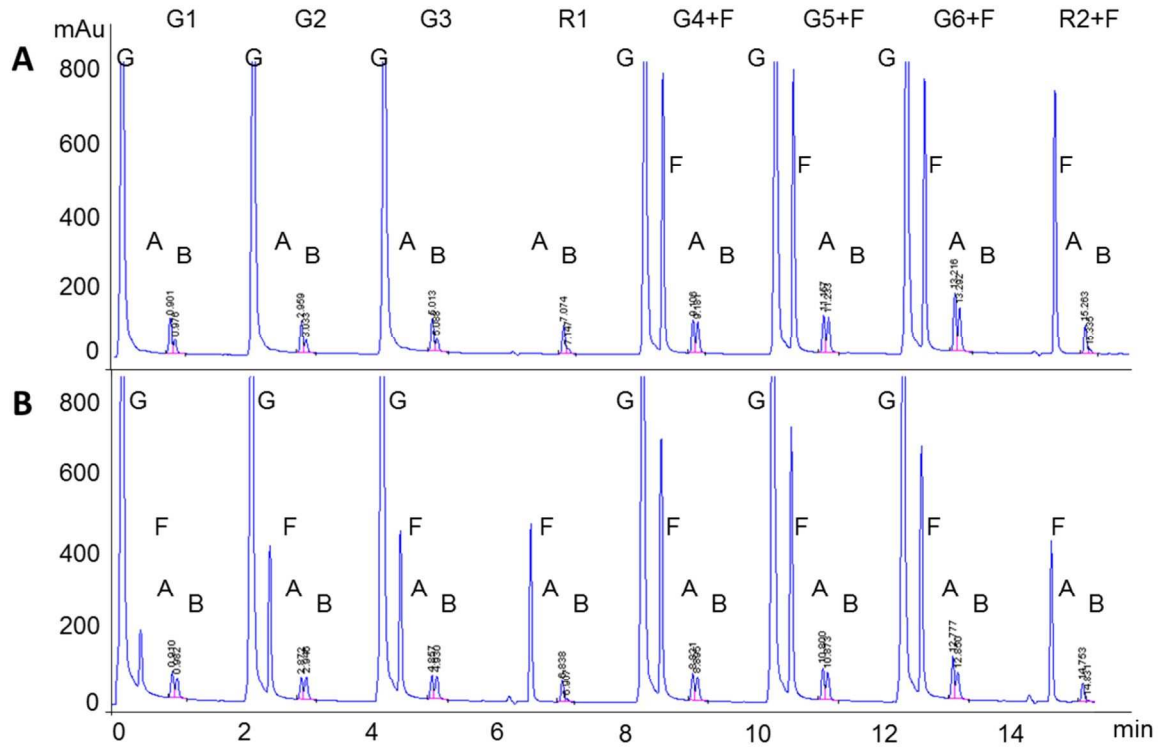

Figure S16: Showing retention time of different species samples in hydrogel (G1-6) and reference (R1-2) containing hydrogel (G, 0.22 min), furan (F, 0.42 min), anisole (A, 0.92 min), benzene (B, 0.99 min) against intensity at 210 nm after A) 9 h, B) 30 h.

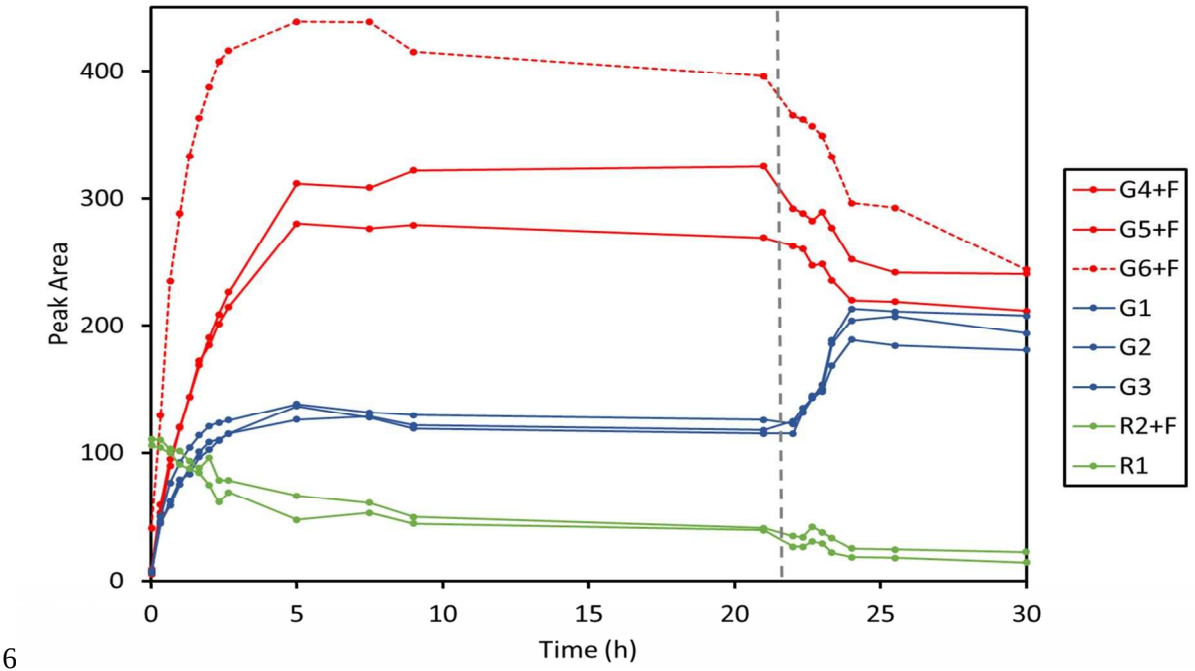

6

Figure S17: Plot showing release of benzene (B) in the presence or absence of the competing guest furan (F) from hydrogels (3 repeats each) and reference solution only samples (RB and RB+F). 1.8 µL of furan or water was injected into the samples after 22 h (indicated by grey line). The xerogel used in the repeat B+F3 (broken red line) was observed to break apart rapidly during reswelling and this repeat was not included in subsequent analysis. The hydrogels were formed from xerogels which had been formed in the presence of an excess of benzene which accounts for the peak area exceeding those of the reference samples.

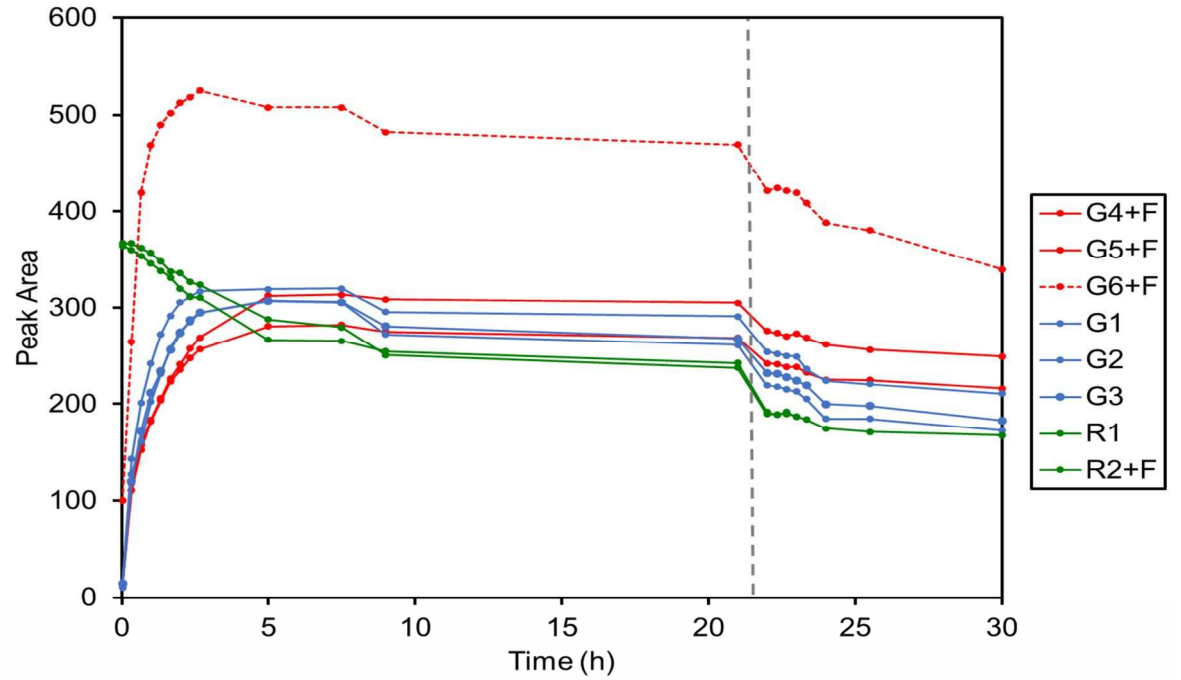

Figure S18: Showing release of anisole (A) in the presence or absence of the competing guest furan (F) from hydrogels (3 repeats each) and reference solution only samples (RB and RB+F). 1.8 µL of furan or water was injected into the samples after 22 h (indicated by grey line). The xerogel used in the repeat B+F3 (broken green line) was observed to break apart rapidly during reswelling and this repeat was not included in subsequent analysis.

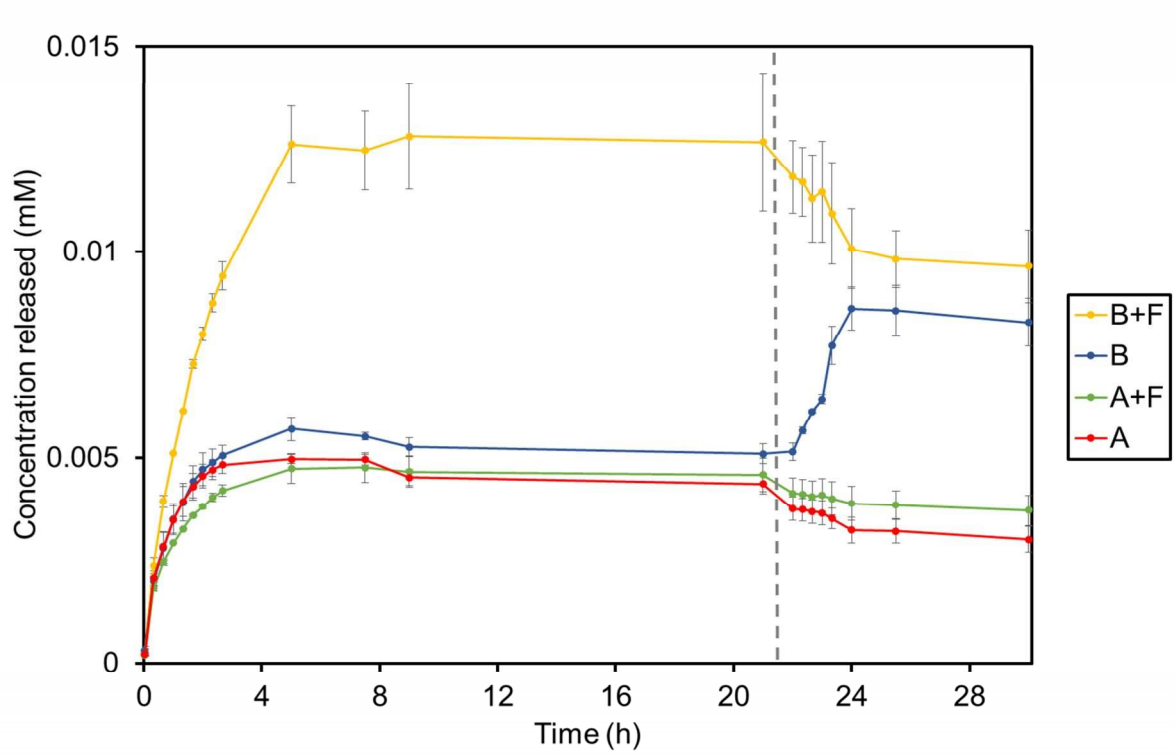

Figure S19: Release profile for benzene (B) and anisole (A) from hydrogels by layering water or furan (F) solutions on top. 1.8 µL of furan was injected into the water samples after 22 h (as indicated by the dashed grey line) and the same volume of water was injected into the furan solution samples.

3.5 Guest release study 2

Separation was achieved on the modular HP1100 HPLC system using an HPLC column (2.7 µm Halo PFP(Pentafluorophenyl), (2.1 × 50 mm) held at 50˚C using a 22% methanol in water mobile phase with a flow rate of 0.9 ml/min and 10 µL injection volume. UV-vis measurements were taken using a UV-Vis detector at wavelengths of 210 nm (8 nm), 217 nm (8 nm), 230 nm (16 nm), 254 nm (16 nm) against a reference at 550 nm (100 nm). Integration of the peak areas of the relevant peaks was undertaken using Agilent ChemStation software (Rev. B.04.01 [481]).

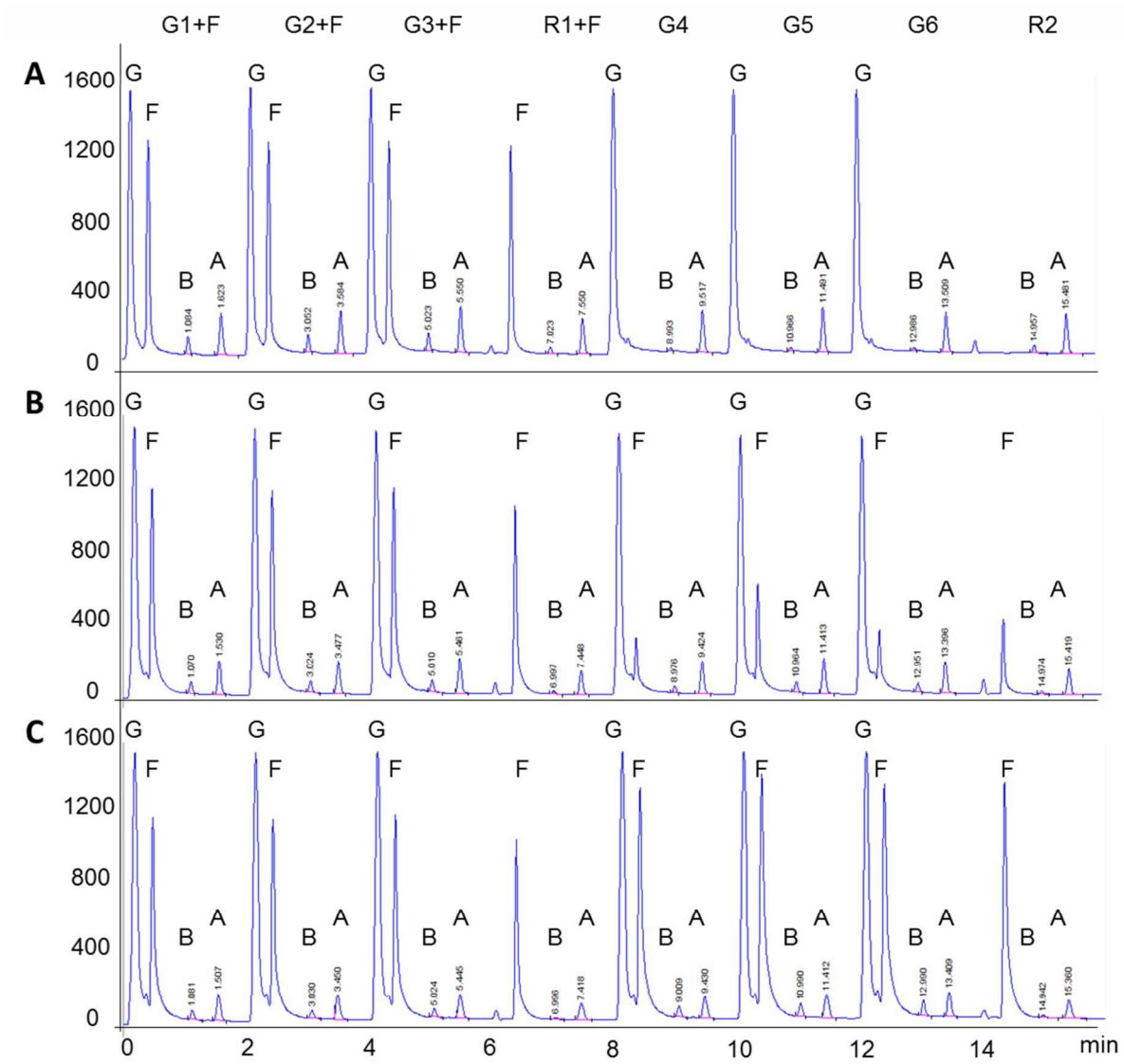

Figure S20: Showing retention time of different species in samples 1-8 for hydrogel (G, 0.15 min), furan (F, 0.44 min), benzene (B, 1.08 min) and anisole (A, 1.50 min) after A) 6h B) 22 h C) 26 h.

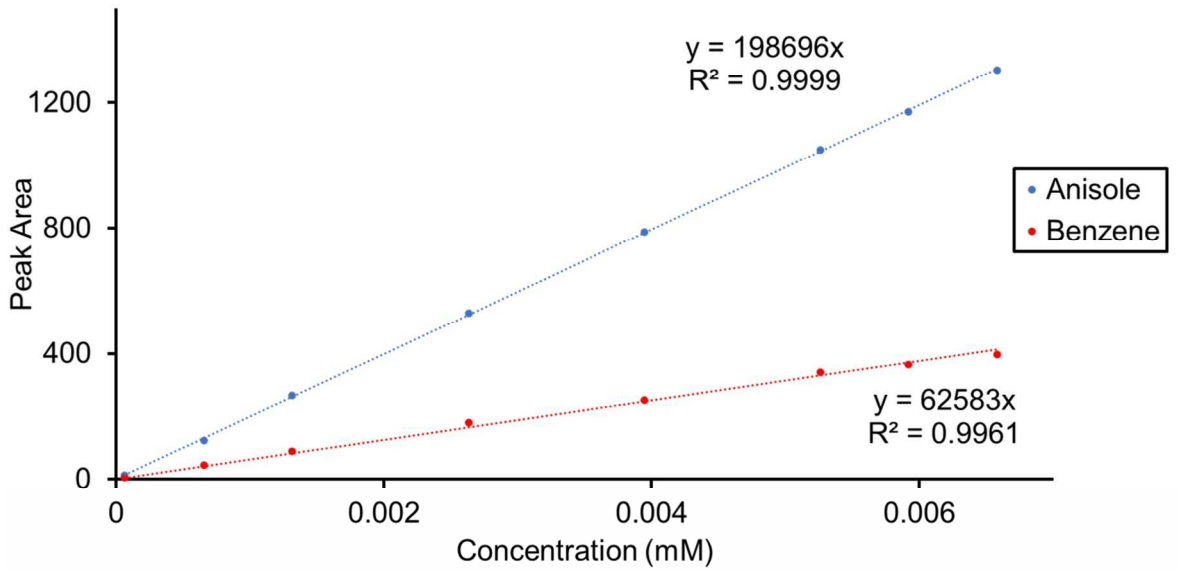

Figure S21: Calibration plot showing peak area at 210 nm against concentration for benzene (blue) and anisole (red) solutions. Correction factors were used to convert peak areas into concentration (mM).

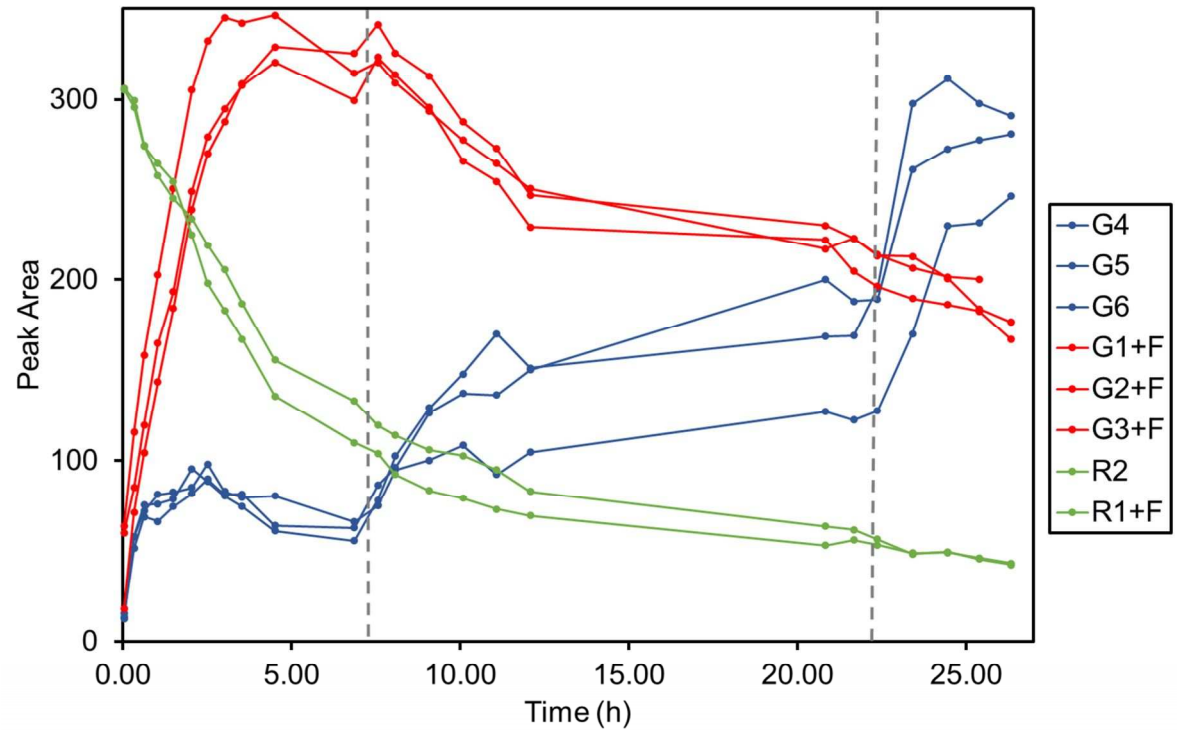

Figure S22: Plot showing release of benzene from hydrogels into water (G4-6) or a furan solution (G1-3+F) along with reference samples containing no gelator (R2 and R1+F). 1 µL of furan was injected into samples (G4-6 amd R2) after 6 h and 1.8 µl was injected after 22 h (as indicated by the dashed grey line) with the corresponding volume of water injected into the remaining samples at the same time intervals.

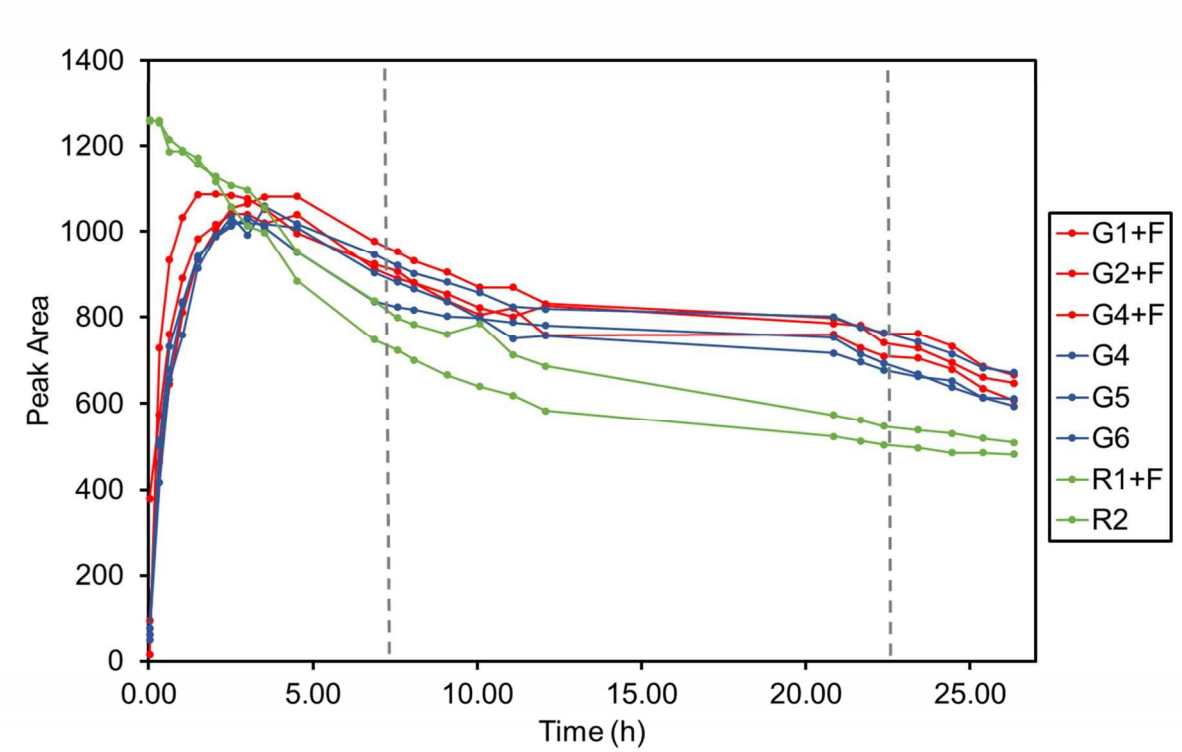

Figure S23: Plot showing release of anisole from hydrogels into water (G4-6) or a furan solution (G1-3+F) along with reference samples containing no gelator (R2 and R1+F). 1 µL of furan was injected into samples (G4-6 and R2) after 6 h and 1.8 µl was injected after 22 h (as indicated by the dashed grey line) with the corresponding volume of water injected into the remaining samples at the same time intervals.

4. Hydrogel Microparticle formation

4.1. Instrumentation

Microparticles were imaged using a Vision Research Phantom Miro EX-4 fast camera with color interpolation, mounted to an Olympus IX-71 inverted microscope (10x-64x objectives). Images were color corrected using Irfanview 4.37 software. The fluorescent label, fluorescein (ex: 488 nm, em: 500-535 nm) were used to track the location of macromolecular dextran cargo (FD, 70 – 500 kDa) within the microdroplet. Fluorescence micrographs were obtained under illumination from a coolLED pE-300white (blue waveband, 450 mW) lamp and imaged with an Olympus IX-81 inverted microscope (Prior proscan II automated stage) mounted with an Andor iXonEM+ DU 897 EMCCD camera, controlled via a PC running custom LabVIEW 2013 software. Fluorescent images were recolored with ImageJ 1.48v software.

4.2. Microfluidic device fabrication

Microfluidic devices were manufactured from polydimethylsiloxane (PDMS) via soft lithography, whereby: (i) the microchannel network was designed in silico (AutoCAD software), (ii) printed as a negative photo-mask and (iii) transferred onto a silicon wafer spin-coated with SU-8 photoresist via UV-photolithography to form a mold. PDMS and the cross linker (Sylgard 184 elastomer kit, Dow Corning) in a 10:1 ratio were poured onto this mold and allowed to stand overnight at 70 °C. The PDMS layer, imprinted with the microfluidic channel design, was removed and using a biopsy punch (1.0 mm) inlets and an outlet were formed. The imprinted PDMS and a glass substrate were exposed to oxygen plasma for 8 s and then pressed together to seal the microfluidic channels.

To render these channels hydrophobic, they were immediately flushed with a 0.5% v/v solution of trichloro(1H,1H,2H,2H-perfluorooctyl)silane in Fluorinert FC-40 (3M) and subsequently cured at 120 °C overnight. This hydrophobic surface-modification was also applied to glass slides that were used in subsequent microparticle studies, insuring low adhesion of microparticles to the surface.

4.3. Microdroplet generation

Monodisperse water-in-oil microdroplets were generated within a hydrophobic flow-focusing microfluidic channel (Figure 5a, S24-S25). The diameter of the junction was 200 µm with a channel depth of 80 µm. To generate microdroplets, the continuous oil phase and the discrete aqueous phase were injected into the microfluidic device via syringe pumps (PHD 2000, Harvard Apparatus) with typical controlled flow rates of 200 and 160 μLh^{-1} respectively. At the intersection, the shear forces caused the formation of aqueous droplets in oil (Ø = 220 µm). The continuous phase comprised of the perfluorinated oil, Fluorinert FC-40 (3M), with 2 wt% surfactant (XL-01-171, Sphere Fluidics). The dispersed phase consisted of a laminar flow of two aqueous solutions (segregating the gel-forming subcomponents) that intersected immediately prior to the flow focus (AQ_1 = AQ_2 = 80 μLh^{-1}). The droplets passed through a winding channel where rapid intra-droplet mixing results in a marked color change from brown to purple, before exiting the microfluidic device through microbore polythene tubing ($Ø_I$ = 380 µm, L = 150 mm).

To form 15 wt% hydrogel microparticles, a solution consisting of iron(II)sulfate heptahydrate (102.59 mg, 4 equiv.) was dissolved in H_2O (4 mL) immediately prior to use (AQ_1). The second solution (AQ_2) was formed by first dissolving tetramethylammonium hydroxide pentahydrate (50.16 mg) in water (1 mL) and using the resulting solution to dissolve 4,4'-diaminobiphenyl-2,2'disulphonic acid (56.45 mg). 0.5 mL of this solution was then used to dissolve of dialdehyde **B (**83.87 mg). It should

be noted that the precipitation of insoluble iron salts within the syringe was observed after several hours; however this could be prevented by preparing the iron solution with 1.0 mM sulfuric acid, with the addition of excess tetramethyl ammonium hydroxide to the PEG/amine solution to compensate.

Control experiments were carried out by replacing either AQ_1 or AQ_2 with water, injected at the same flow rate so that the size and composition of the microdroplet was otherwise unaffected.

For cargo release studies, a microfluidic device where three aqueous inputs intersected at a single flow-focusing junction (120 x 80 µm) was used to introduce a third 'cargo' flow independently to gel-forming components. As shown in Figure S35, the first cross-junction (80 x 80 µm) brings together the three aqueous solutions into a single laminar flow, with the central aqueous 'cargo' solution used to inhibit gelation at the water/water interface. The second cross-junction (120 x 80 µm) then acts as a flow focus, where aqueous microdroplets are generated on intersection with perpendicular oil flows. Here typical flow rates of AQ_{tot} = 200 μLh^{-1} and Oil = 100 μLh^{-1} gave rise to 200 µm diameter microdroplets. The composition and relative flow rates of the three aqueous solutions were adjusted to retain a 15 wt% loading within the resultant mixed microdroplet.

Once formed, gelled microdroplets were collected on to the surface of a glass slide for further study, with the aqueous phase allowed to slowly evaporate at RTP to form dry microparticles. Alternatively gelled microdroplets could be stored as a suspension in oil within a sealed vial for several weeks, prior to evaporation. Residual surfactant was removed from dry microparticles by washing with fluorinated solvent (HFE-7100) prior to further study.

4.4. Microparticle analysis

All aqueous solutions were prepared in deionized water (Millipore Milli-Q Gradient A10) ensuring a resistivity of >15 $M\Omega cm^{-1}$.

Microparticle hydration was carried out in deionized water, or with an aqueous solution of (i) tris(2-aminoethyl)amine, (ii) p-toluenesulfonic acid or (iii) 2-formylpyridine – all known to trigger disassembly of cage **1**.

4.5. Cargo release studies

Fluorescein isothiocyanate-dextrans (FD) are most widely used for investigating the permeability and transport in cellular and tissue membranes on account of their biocompatibility, low toxicity and the provision of fluorescence-based quantitative data. FD with molecular weights greater than 5 kDa behave as a flexible and extended coil in solution and hence it is reasonable to consider each with a different Stoke's radius, or hydrodynamic radius. This parameter denotes the radius of a theoretical hard sphere that diffuses at the same rate as the molecule, and is often used in defining the spatial size of FD and hence in inferring the pore size of a material.

FD with molecular weights of 70, 150, 250 and 500 kDa were loaded into the microparticles during formation (as described in Section 4.3 and in Figure S35) to investigate the porosity of the hydrogel and to demonstrate triggered release of cargo. For porosity studies, a high loading of FD (3.0 mg/mL within the mixed droplet) was required due to due to the strong absorption by the purple cage complex at the emitted wavelength. However, it was observed that high loadings of macromolecular cargo dramatically retarded the cage disassembly process and consequentially a lower FD loading of 1.0 mg/mL was used for triggered release studies (Figure 6). It should be noted that in the latter case, the appearance of a ring in the fluorescence micrograph does not reflect the distribution of fluorescent cargo within the microparticle but is due to this intense absorption.

Porosity. The microdroplet precursors were dehydrated to generate stable microparticles and the localization of the fluorescein dye was verified using fluorescence microscopy. The dried gel microparticles were redispersed in in deionized water (20 µL) and fluorescence micrographs were collected over the course of one hour at 1 min intervals. As with the unloaded microparticles, initial wetting resulted in swelling, with a significant increase in diameter over the first minute. Further gradual swelling was then observed for up to ten minutes post wetting. During this swelling period microparticles loaded with 70 and 150 kDa FD were observed to release their cargo into the bulk media (Figure S36). In contrast, only a small amount of cargo was observed to release from microparticles loaded with 250 kDa FD, potentially limited to cargo held near the surface, and no release was observed from microparticles containing 500 kDa FD. After this diffusive release upon initial swelling, the release of remaining cargo of all molecular weights was too slow to be quantified over the timescale of the experiment. In contrast to the unloaded microparticles (Figure S28), no further swelling was observed this timescale. Based on the corresponding Stoke's radii, these microparticles are estimated to have a hydrated pore diameter between 17-21 nm.

Triggered release. As shown in Figure 4, the hydration of microparticles loaded with 500 kDa FD (1.0 mg/mL) in deionized water (20 µL) resulted in swelling, but little loss of cargo. The subsequent addition of 20 µL 0.1 M p-toluenesulfonic acid was then used to trigger release of cargo. This process proceeded more slowly for loaded than for unloaded microparticles (Figure S32-33). Release of fluorescent cargo from the microparticles was observed after two minutes, but it required a further four minutes for the microparticles to completely dismantle with corresponding release of all FD cargo into the surrounding media.

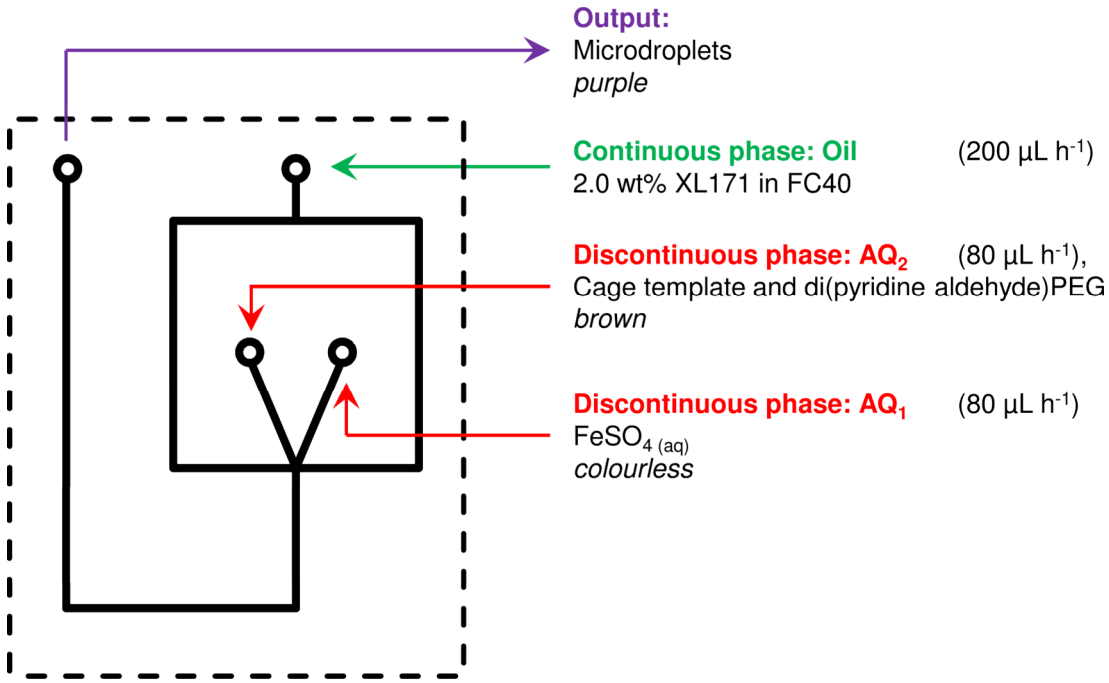

Figure S24: Schematic of the microfluidic device, showing the composition and flow rate of the different solutions injected into the microfluidic device, as shown in Figure S25.

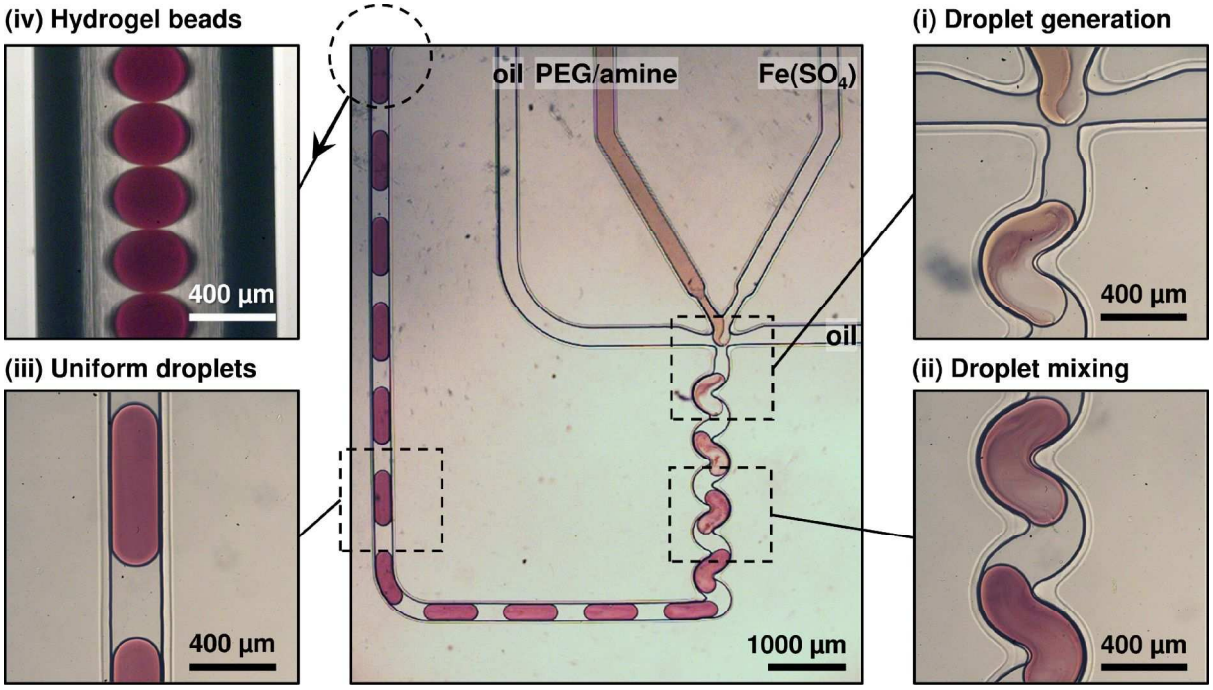

Figure S25: Transmission optical micrograph of the generation of monodisperse water-in-oil microdroplets at a 200 µm microfluidic flow-focusing junction, highlighting: (i) microdroplet generation, (ii) rapid mixing of reagents within the droplet, (iii) uniformly-mixed purple microdroplets and (iv) gelation to form microparticles as they flow along the exit tubing (Ø = 380 µm).

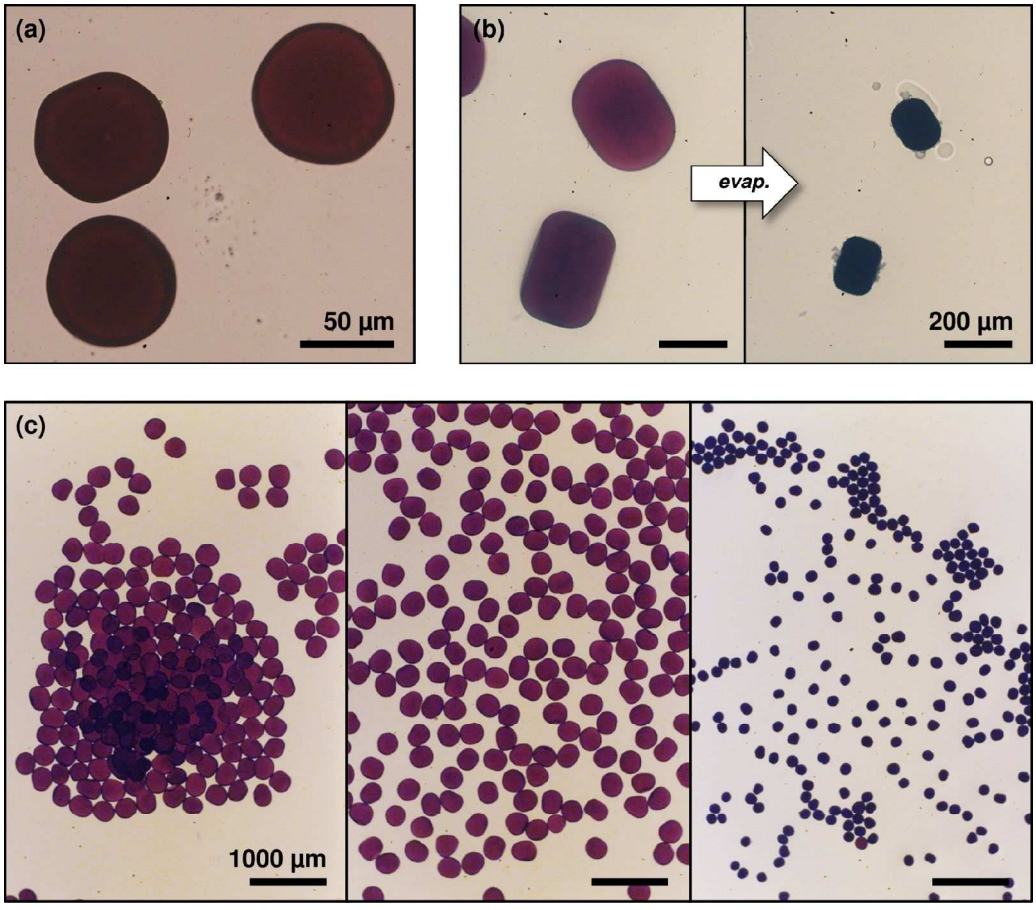

Figure S26: Transmission optical micrographs indicative of hydrogel formation within the microfluidic device: **(a)** Upon exiting the microbore tubing non-spherical microparticles with 'dents' from collision with other

particles were observed. **(b)** Altering the relative flow rates (AQ_{tot} = 100, Oil = 100 µLh^{-1}) allowed for much larger microdroplets to be formed that were spatially constricted within the microfluidic channels. This resulted in spherocylinder-shaped microparticles (left), upon evaporation this shape was retained (right). **(c)** Deposition of a large number of hydrogel microparticles at a single point would result in a heap or pile (left) – in stark contrast to liquid microdroplets, which tend to reflow into a hexagonal close-packed array. Addition of oil allows the microparticles to be suspended, allowing the high monodispersity of the particle sizes to be seen, both initially (center) and once dry (right).

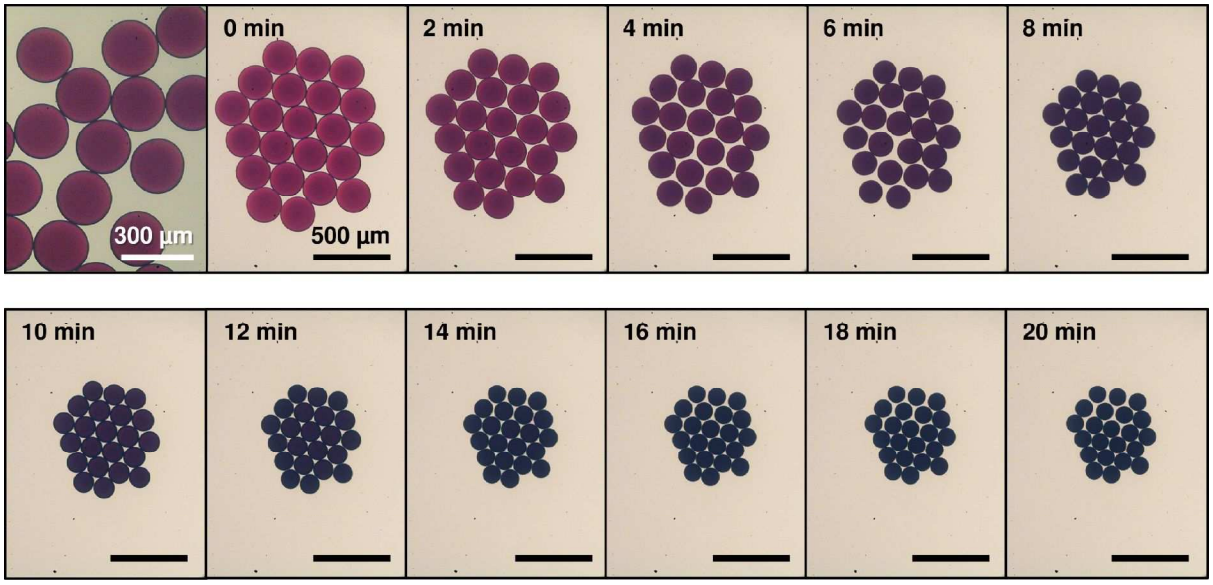

Figure S27: Transmission optical micrographs of the evaporation of water from the hydrogel microparticles, over 20 minutes.

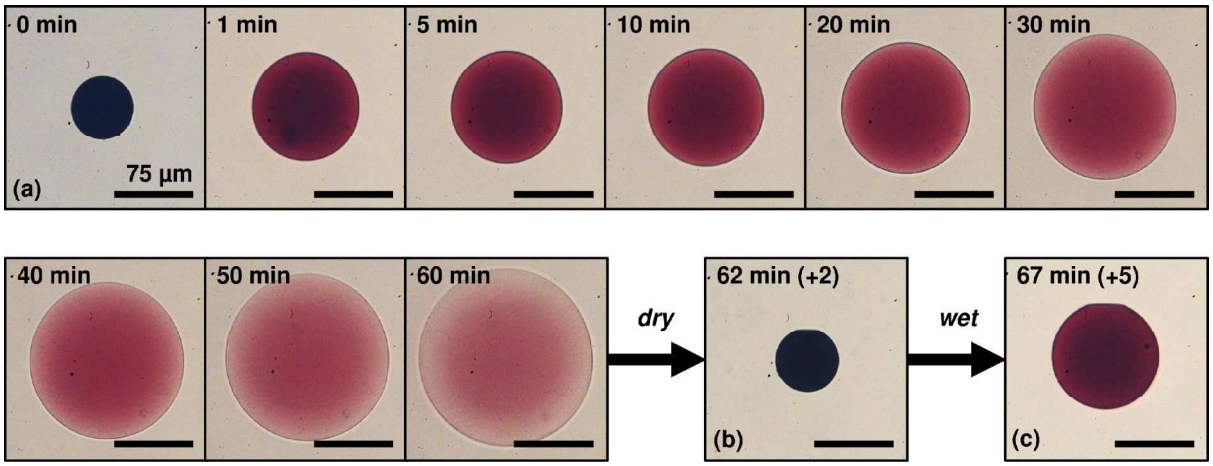

Figure S28: (a) Transmission optical micrographs of the hydration a dry microparticle in deionized water (25 µL), over 60 minutes. **(b)** Evaporation restores the hydrogel microparticle to the original collapsed state. **(c)** Subsequent rehydration (+5 mins) reinstates the microparticle to the swollen state. Scale bars are 75 µm.

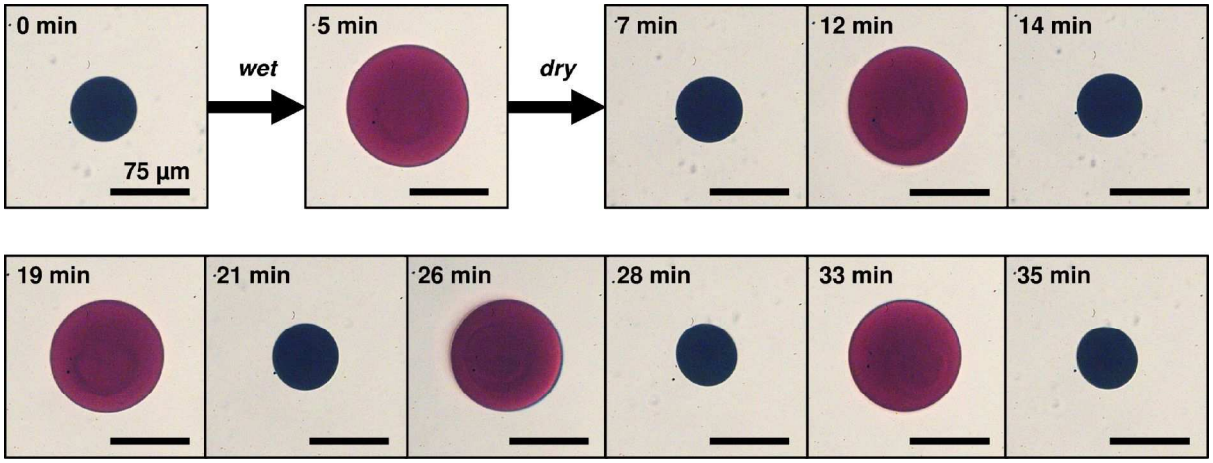

Figure S29: Transmission optical micrographs of the repeated hydration in deionized water (10 µL, 5 min) and evaporative drying (2 min) of a hydrogel microparticle, over 35 minutes. Scale bars are 75 µm.

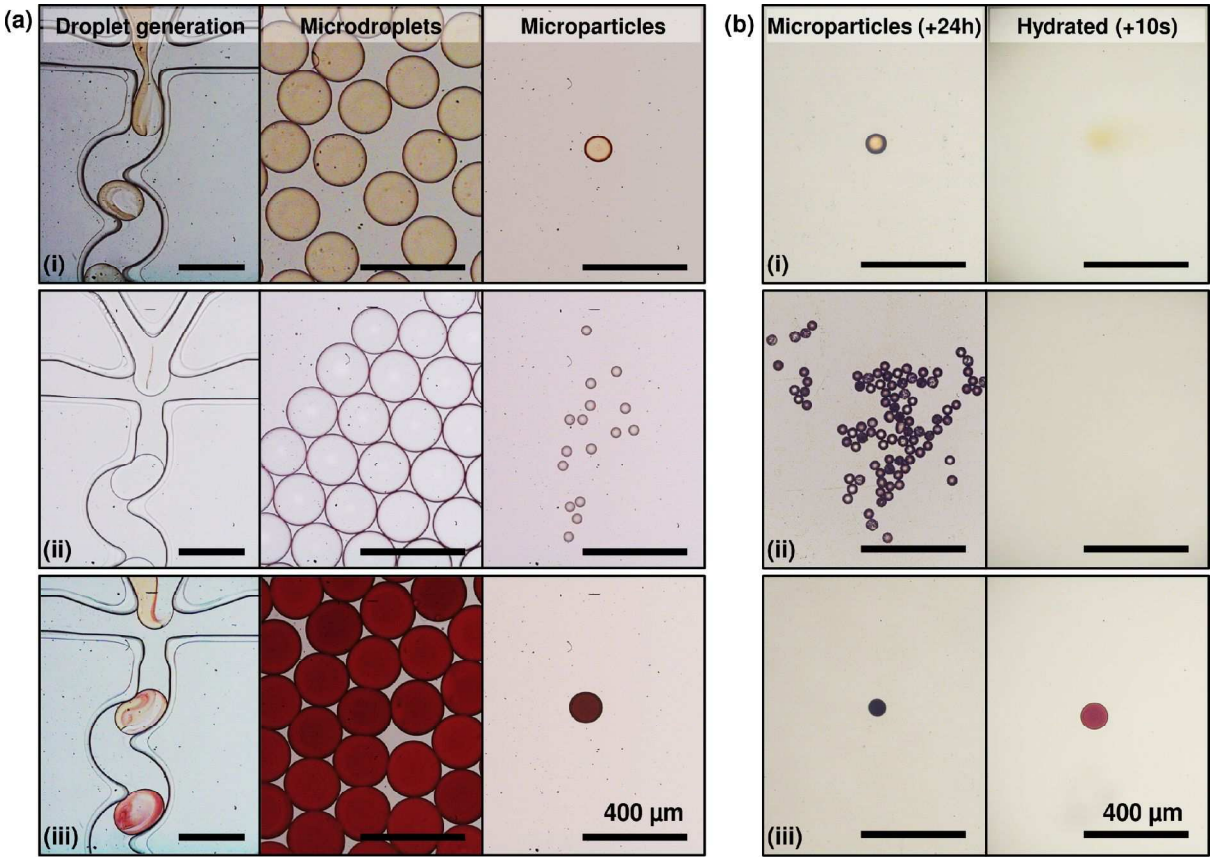

Figure S30. (a) Transmission optical micrographs of microdroplet generation (left) and subsequent evaporation (right) for controls: (i) PEG/amine only and (ii) iron(II) sulfate only, and in contrast with (iii) the 1:1 mixed system. **(b)** Hydration of dried microparticles in deionized water (10 µL) resulted in rapid dissolution of both 'controls', with only the mixed system forming stable hydrated microparticles. Scale bars are 400 µm.

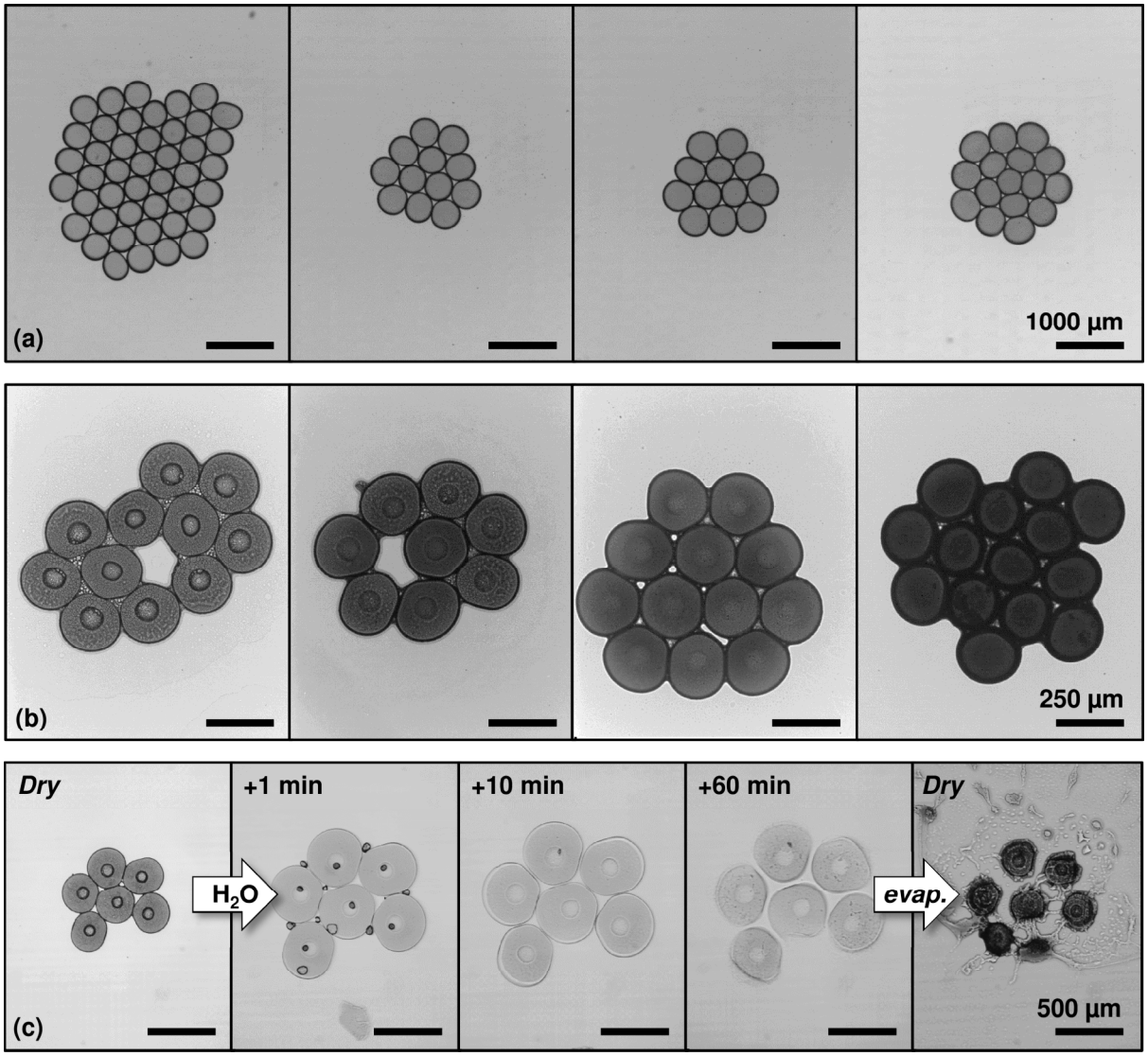

Figure S31: (a,b) Transmission optical micrographs showing microdroplets containing (left to right) 5.0, 7.5, 10 and 15 wt% of subcomponents as (a) initially collected hydrogel microparticles and (b) after evaporation. At lower loadings the microparticles are unable to retain their shape upon evaporation, with 5.0 and 7.5 wt% forming flattened disks. **(c)** Hydration of 5.0 wt% dry microparticles with deionized water, following storage for 11 days on the glass slide at room temperature.

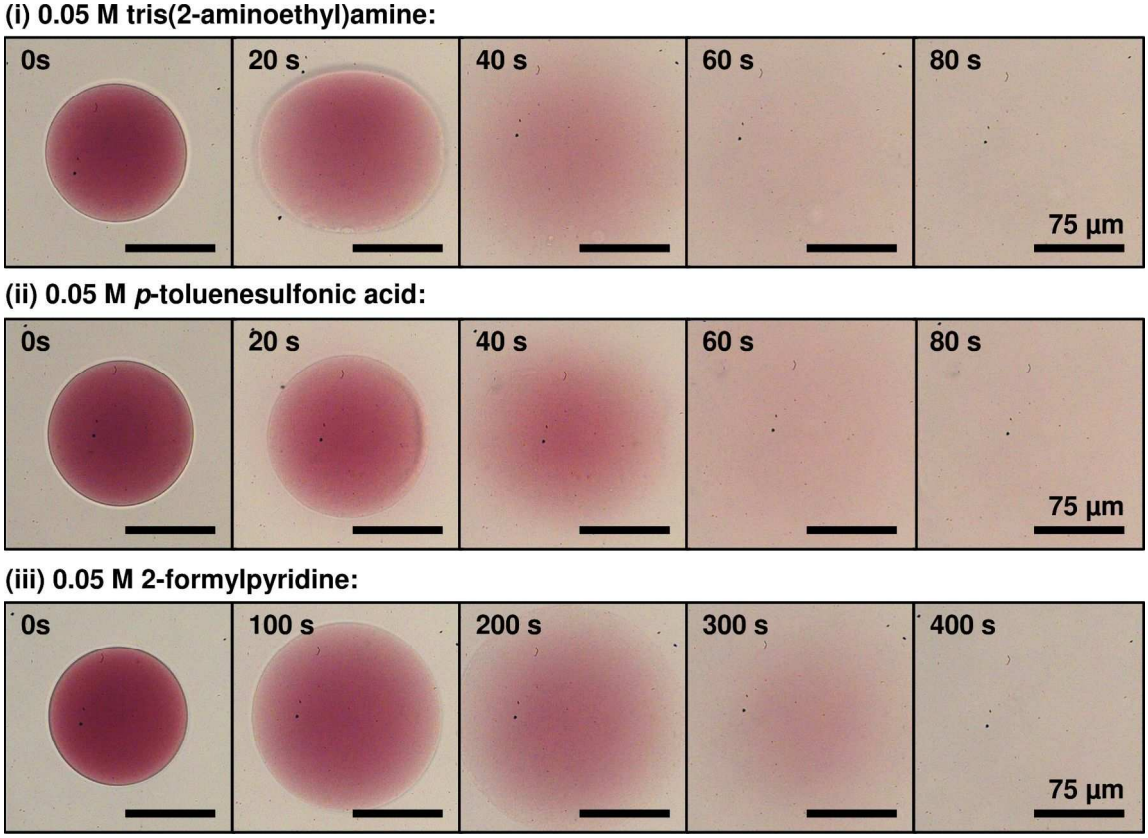

Figure S32: Transmission optical micrographs of the swollen hydrogel microparticle, hydrated in deionized water (2 µL, 10 mins). On further addition of 2 µL of a 0.1 M aqueous solution of: (i) tris(2-aminoethyl)amine, (ii) p-toluenesulfonic acid or (iii) 2-formylpyridine, rapid disassembly the cage-linked hydrogel is observed, with acid/amine observably noticeably faster. Scale bars are 75 µm.

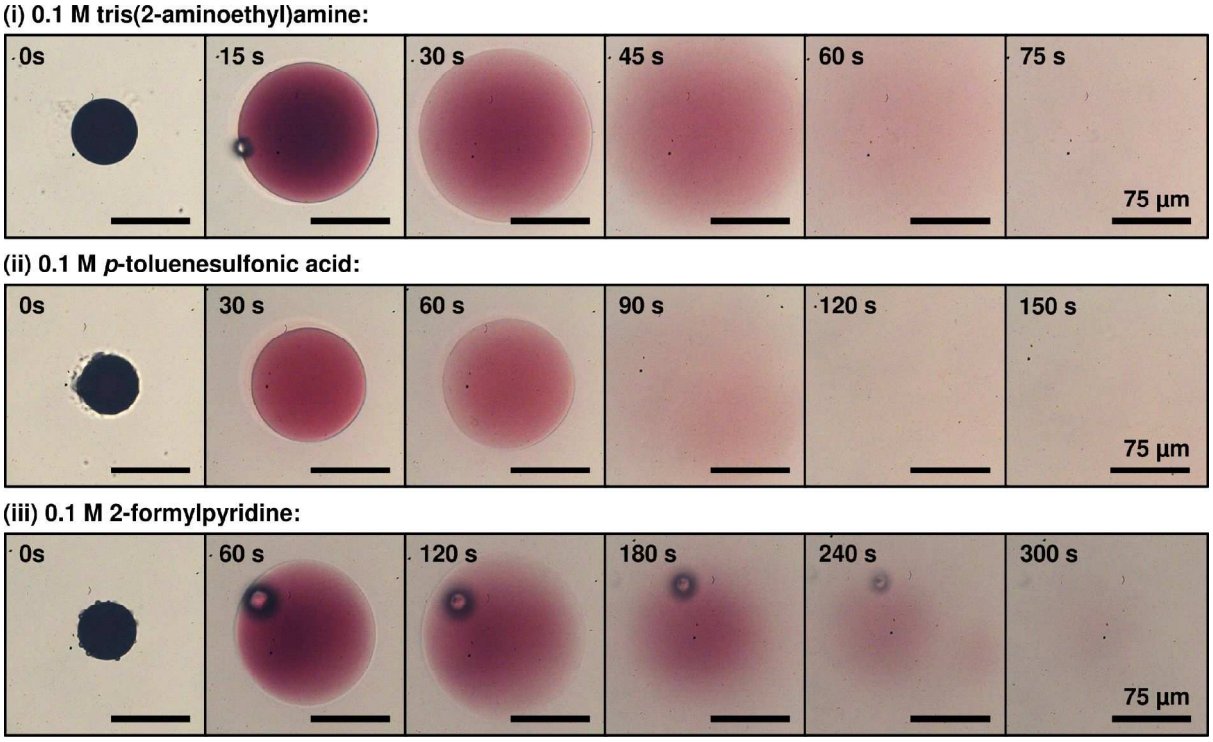

Figure S33: Transmission optical micrographs of the hydration a dry microparticle with 2 µL of a 0.1 M aqueous solution of: (i) tris(2-aminoethyl)amine, (ii) p-toluenesulfonic acid or (iii) 2-formylpyridine. All three

solutions result in disassembly the cage-linked hydrogel, with amine substitution observably faster than acid and displacement of the aldehyde the slowest. N.b. The dark region observed in (iii) is an air bubble trapped under the microparticle. Scale bars are 75 µm.

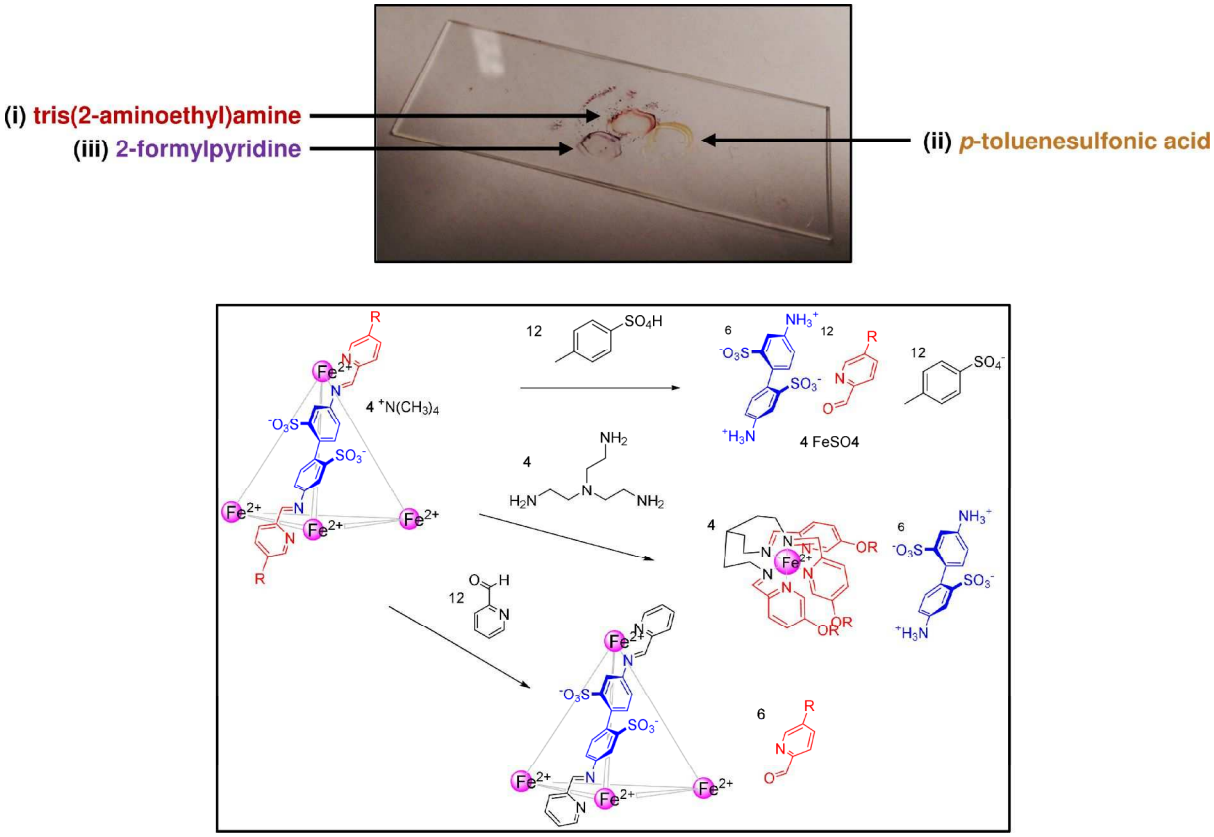

Figure S34: Photograph of the glass slide after treatment of the hydrogel microparticles with 0.1 M aqueous solutions of: (i) tris(2-aminoethyl)amine, (ii) p-toluenesulfonic acid or (iii) 2-formylpyridine. The different colors observed correlate with the expected disassembly products that result from the different mechanisms of as described in the scheme below.

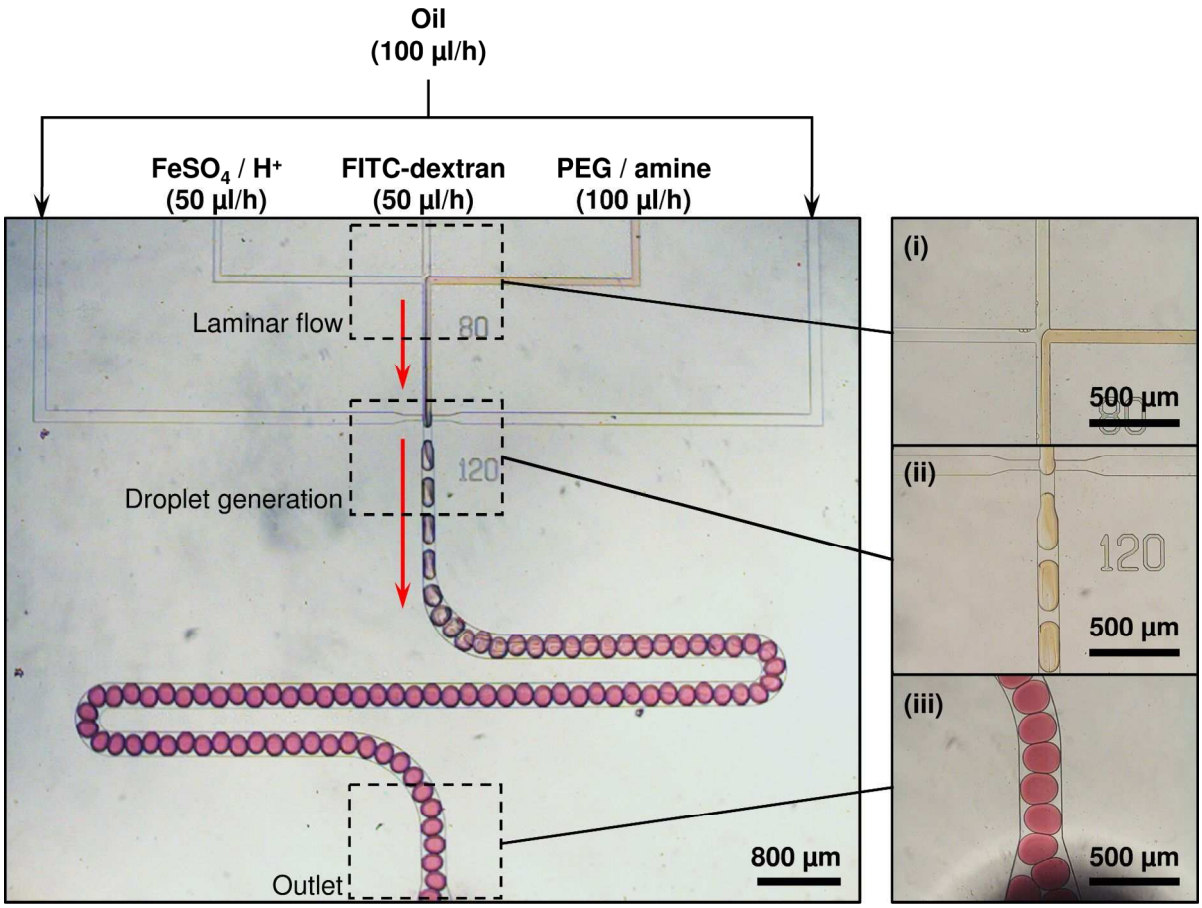

Figure S35: Transmission optical micrograph of microfluidic device used for generating cargo-loaded hydrogel microparticles. (i) The first cross-junction (80x80 µm) brings together the three aqueous solutions into a single laminar flow, with the central aqueous 'cargo' solution used to inhibit gelation at the water/water interface. (ii) The second cross-junction (120x80 µm) acts as a flow focus, where aqueous microdroplets are generated on intersection with perpendicular oil flows. Rapid intra-droplet mixing occurs resulting in a marked color change from brown to purple. (iii) At the outlet of the device the monodisperse water-in-oil droplets are uniformly colored, with gelation continuing along the exit tubing (Ø = 380 µm).

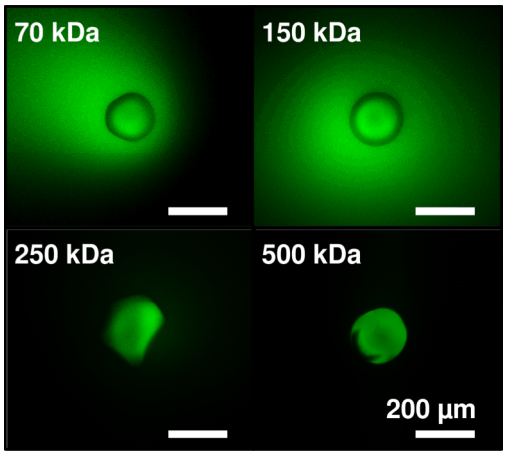

Figure S36. Fluorescence micrographs of hydrogel microparticles containing FITC-dextran macromolecular cargo (70 – 500 kDa, 3.0 mg/mL). After hydration in deionized water for 10 minutes, with corresponding swelling, fluorescein isothiocyanate-dextran (FD) cargo below 150 kDa was observed to release into bulk media. In contrast higher molecular weight cargo is retained. Scale bars are 200 µm.

4.6. Scanning electron microscopy of microparticles

Hydrogel microparticles were deposited from fluorinated oil, washed with FC60 and either freeze dried or dried under vacuum before sputter coating with platinum (40 mA, 0-20 s). Longer coating times resulted in the build-up of a skin of platinum which masked finer features, however, the resolution of images taken with lower coating times were inhibited by the build-up of charge.

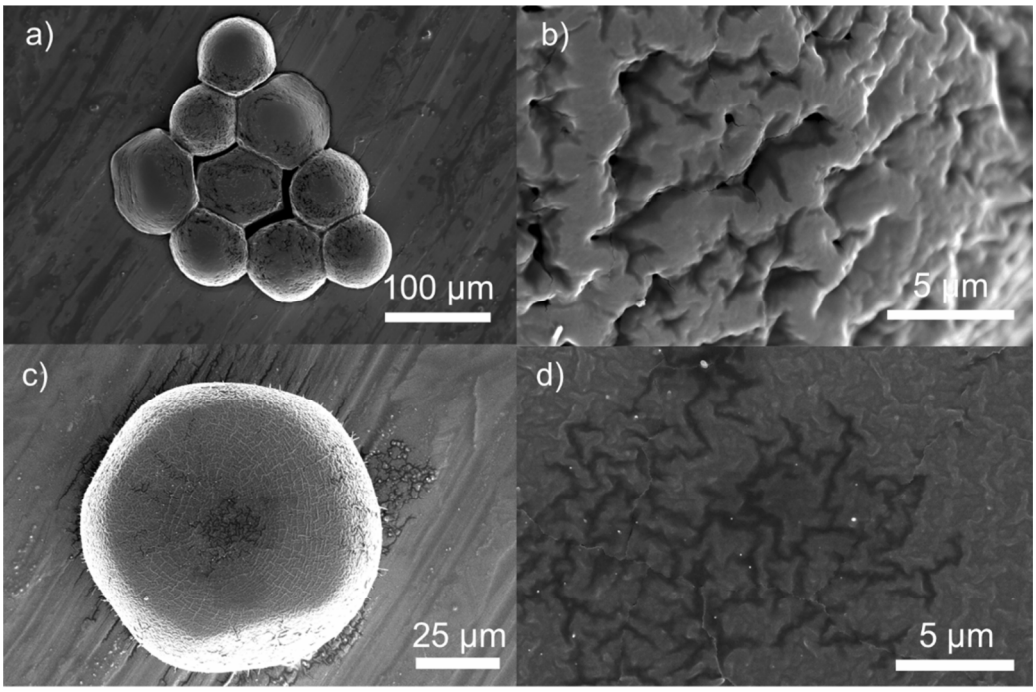

Figure S37: SEM image showing 15 wt% hydrogel microparticles prepared by freeze drying (top row) or drying under vacuum (bottom row) prior to coating with platinum.

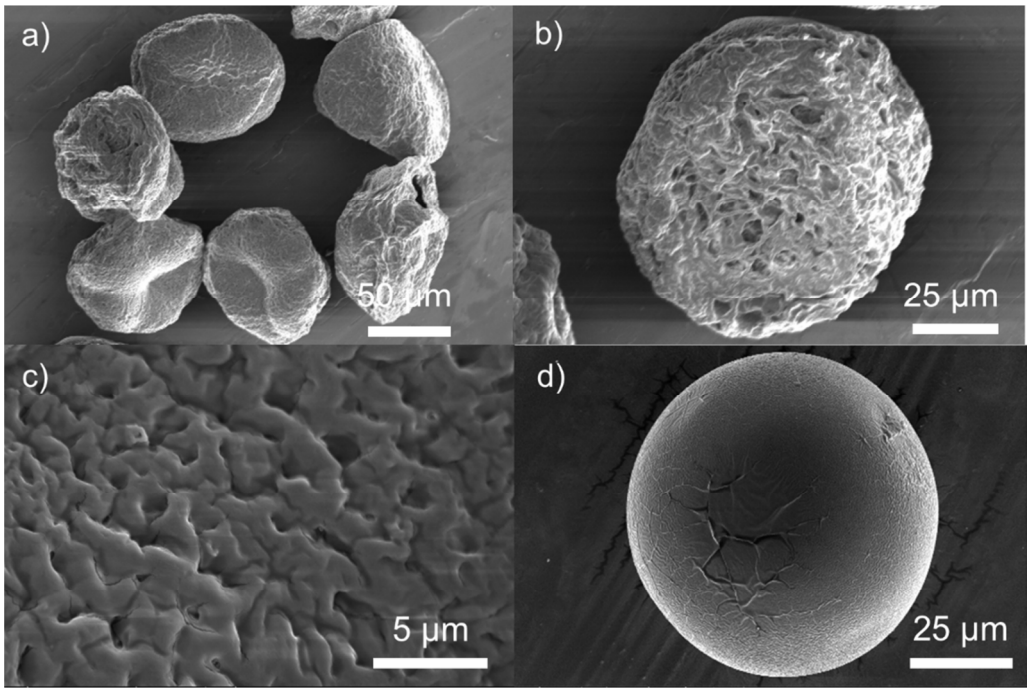

Figure S38: SEM image showing 15 wt% hydrogel microparticles containing 500 KDa fluorescein tagged dextran prepared by freeze drying (a-c) or drying under vacuum (d) prior to coating with platinum (40 mA, 20 s).